




Review

Status and Perspectives on Rare Decay Searches in Tellurium Isotopes

Alice Campani ^{1,2,†} , Valentina Dompè ^{3,4,†}  and Guido Fantini ^{3,4,*,†} ¹ Dipartimento di Fisica, Università di Genova, I-16146 Genova, Italy; alice.campani@ge.infn.it² INFN—Sezione di Genova, I-16146 Genova, Italy³ Dipartimento di Fisica, Sapienza Università di Roma, I-00185 Roma, Italy; valentina.dompe@uniroma1.it⁴ INFN—Sezione di Roma, I-00185 Roma, Italy

* Correspondence: guido.fantini@uniroma1.it

† These authors contributed equally to this work.

Abstract: Neutrinoless double beta decay ($0\nu\beta\beta$) is a posited lepton number violating decay whose search is an increasingly active field in modern astroparticle physics. A discovery would imply neutrinos are Majorana particles and inform neutrino physics, cosmology and beyond-standard-model theories. Among the few nuclei where double beta decay ($\beta\beta$) is allowed, tellurium isotopes stand for their high natural abundance and are currently employed in multiple experiments. The search for $0\nu\beta\beta$ will provide large exposure data sets in the coming years, paving the way for unprecedented sensitivities. We review the latest rare decay searches in tellurium isotopes and compare past results with theories and prospects from running experiments.

Keywords: double beta decay; tellurium; ^{120}Te ; ^{123}Te ; ^{128}Te ; ^{130}Te



Citation: Campani, A.; Dompè, V.; Fantini, G. Status and Perspectives on Rare Decay Searches in Tellurium Isotopes. *Universe* **2021**, *7*, 212. <https://doi.org/10.3390/universe7070212>

Academic Editor: Clementina Agodi

Received: 31 May 2021

Accepted: 23 June 2021

Published: 26 June 2021

Publisher's Note: MDPI stays neutral with regard to jurisdictional claims in published maps and institutional affiliations.



Copyright: © 2021 by the authors. Licensee MDPI, Basel, Switzerland. This article is an open access article distributed under the terms and conditions of the Creative Commons Attribution (CC BY) license (<https://creativecommons.org/licenses/by/4.0/>).

1. Introduction

Double beta decay is a rare second order standard model (SM) weak interaction process where a nucleus transforms into a member of the same isobaric multiplet. The investigation of rare decays is an active topic of research.

The interest in double beta decay emitter nuclei is driven by the search for the beyond-SM (BSM) process of neutrinoless double beta decay ($0\nu\beta\beta$) and has led to date to the collection of large data samples of decays in increasingly low background conditions [1]. The discovery of $0\nu\beta\beta$ decay would demonstrate at once that lepton number is not conserved, that neutrinos are particles endowed with Majorana mass and would provide precious information on their mass scale and ordering [2,3]. In addition, such data allow for precision measurement of $\beta\beta$ decay half lives, whose importance is not restricted to updating results on nuclear spectroscopy. In fact, exact calculations of the nuclear dynamics are not available for heavy nuclei as the ones that undergo $\beta\beta$ decay, and one must rely on effective theories. Comparing theoretical predictions and measurements of decay rates in different modes and emitters will validate and qualify the nuclear matrix element (NME) calculations currently available [4,5]. This in turn would allow one to extract an estimate of the effective Majorana mass ($m_{\beta\beta}$) from a measurement (or a limit) of the $0\nu\beta\beta$ decay rate. At present, limits on $m_{\beta\beta}$ suffer from a dominant uncertainty due to the spread of NME results among different models. Indications exist that the axial–vector coupling constant in heavy nuclei is quenched with respect to its free nucleon value [6]. In addition, BSM models such as $\beta\beta$ decay with Majoron emission can be searched for with the same data [7].

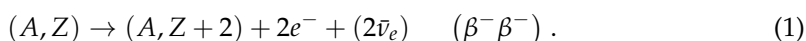
Significant insights can be extracted from the current experimental program of Te $\beta\beta$ searches. This motivates a review of the most recent results available for each possible mechanism. The structure of this work is outlined in the following: Section 2 is devoted to a phenomenological overview of double beta decay. After a general description of the most relevant features of the SM allowed mechanisms ($2\nu\beta\beta$, $EC\beta^+$, ECEC), we introduce their

lepton number violating counterparts. In Section 3, we give an approximate analytical formula for the sensitivity of peak searches and summarize the most relevant experimental techniques employed for $\beta\beta$ searches in tellurium. The following part of this article is specifically devoted to the isotopes of Te where rare decay modes are energetically allowed and currently investigated. We discuss the ones with a half life longer than the age of the universe. In Sections 4–7, we highlight the most relevant results for rare decay modes of ^{130}Te , ^{128}Te , ^{123}Te and ^{120}Te , respectively. We try to include, whenever available, preliminary results released by experimental groups involved in such analyses in order to provide an insight on the work that is currently ongoing in this field of research and its potential in the next years. Finally, we summarize our conclusions in Section 8.

2. Double Beta Decay

Double beta decay ($\beta\beta$) is a spontaneous weak process changing the nuclear charge Z by two units while leaving the atomic mass A unchanged. It is a transition among isobaric isotopes. Having in mind the Weizscker mass formula [8], it is evident that the most suitable candidate isotopes for the study of $\beta\beta$ decay are even–even nuclei, for which single β decay is energetically forbidden. The transition can proceed both to the ground state or to the first excited states of the daughter nucleus.

The mechanism with the highest expected rates is $\beta^-\beta^-$:



The 2ν -mode was theorized by M. Goeppert-Mayer [9] in 1935 and can be seen as two simultaneous neutron decays. Even if strongly suppressed, it has been observed in 12 nuclei with half lives ranging from about 10^{19} yr to 10^{24} yr [10].

An alternative mode where the anti-neutrinos are not emitted was later proposed by W. H. Furry [11], who called it *neutrinoless double beta decay* ($0\nu\beta\beta$). The main feature of the $0\nu\beta\beta$ transition is the explicit violation of the lepton number (L) by two units. The discovery of $0\nu\beta\beta$ decay would provide a direct indication of physics BSM. Moreover, this observation could be linked to the cosmic asymmetry between matter and antimatter (baryogenesis via leptogenesis [12]).

In the attempt to investigate the nature of $0\nu\beta\beta$ decay, various theoretical possibilities were considered and many extensions of the SM include mechanisms that can explain it [13–20]. However, the general interest has always remained focused on the neutrino mass mechanism. This scenario is supported by two important facts:

- On the theoretical side, the simplest operator that obeys the gauge symmetry $SU_C(3) \otimes SU_L(2) \otimes U_Y(1)$ but violates L is the one that generates a Majorana mass for neutrinos, thereby providing a possible origin of the smallness of neutrino masses;
- On the other hand, the experiments with solar, atmospheric, reactor and accelerator neutrinos have provided compelling evidence for the existence of neutrino oscillations [21], thereby requiring neutrinos to be massive particles.

Therefore, the $0\nu\beta\beta$ decay is also a key tool for studying neutrinos. From now on, we will analyze this transition assuming the light Majorana neutrino exchange.

Taking into account the nuclear dynamics, the half life¹ for the $2\nu\beta\beta$ mode can be factorized as

$$[T_{1/2}^{0\nu}]^{-1} = \mathcal{G}_{2\nu}(Q, Z) |\mathcal{M}_{2\nu}|^2 \tag{2}$$

where $\mathcal{G}_{2\nu}(Q, Z)$ is the invariant phase space factor (PSF) of the decay and represents the kinematic contribution to $2\nu\beta\beta$, namely it accounts for the different ways the total energy available in the reaction can be split among all the particles in the final state. $\mathcal{M}_{2\nu}$ is the nuclear matrix element (NME) and accounts for the relevant nuclear structure aspects of the process. Considering the $0\nu\beta\beta$ mode, the most general expression for the half life is

$$[T_{1/2}^{0\nu}]^{-1} = \mathcal{G}_{0\nu}(Q, Z) |\mathcal{M}_{0\nu}|^2 |f(m_i, U_{ei})|^2 \tag{3}$$

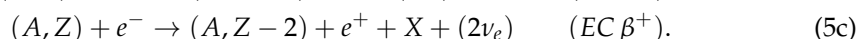
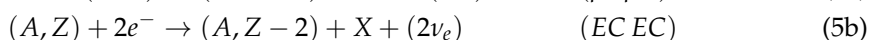
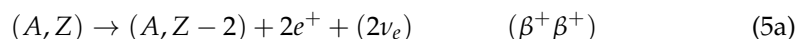
where $f(m_i, U_{ei})$ represents the BSM contribution to the decay, a function of the neutrino masses m_i and mixing matrix elements U_{ei} of the neutrino species. Assuming the three neutrino mixing scheme, f is parameterized as follows:

$$f(m_i, U_{ei}) = \frac{m_{\beta\beta}}{m_e} = \frac{1}{m_e} \left| e^{i\eta_1} |U_{e1}^2| m_1 + e^{i\eta_2} |U_{e2}^2| m_2 + |U_{e3}^2| m_3 \right|. \tag{4}$$

$m_{\beta\beta}$ is called the *effective Majorana mass* and can be conceived as the electron neutrino mass that rules the $0\nu\beta\beta$ transition, while η_1 and η_2 indicate the Majorana phases. Inverting Equation (3), an experimental lower limit on the half life can be translated into a limit on the effective Majorana mass. However, since the Majorana phases cannot be probed by oscillation experiments, the allowed regions for $m_{\beta\beta}$ are obtained by letting them vary freely.

Both the PSF and the NME that govern the decay must be accurately calculated if experiments are to reach their full potential. The theory behind $G_{0\nu}$ is well known, and precise calculations have been carried out by many authors [22], the largest difficulties being related to computational issues. It generally scales as the fifth power of the Q-value of the transition. The present uncertainty on phase space factors is dominated by the uncertainty on the Q-value and is around 7%. Instead, only approximate estimates of the NME have been so far obtained, due to the many body nature of the nuclear problem. A detailed overview of the existing approaches to the evaluation of NME is presented in [5] and references therein.

To date, we have described the most promising mode of double beta decay. However, other interesting forms of SM $\beta\beta$ decay exist. Depending on the relative numbers of the nucleus protons and neutrons, three additional mechanisms are possible:



For the sake of clarity, β^- (β^+) indicates the emission of an electron (positron) and EC stands for electron capture. X represents X-rays or Auger electrons emitted in the electron capture process. In parentheses we indicate the $\nu_e/\bar{\nu}_e$ emitted in the SM counterpart of each transition. There are 34 candidate emitter nuclei for these decays. Only 6 nuclei can undergo all the above mentioned processes, 16 nuclei can undergo $\beta^+ EC$ and $ECEC$, while 12 can undergo only $ECEC$.

In the following, we briefly review the scientific motivations underlying the study of each double beta decay mode. While $\beta^- \beta^-$ decays have the largest expected rates, the different decay topology could help in the identification of the underlying mechanism of $0\nu\beta\beta$ transition, in case this will finally be observed.

2.1. Double Electron Decay ($\beta^- \beta^-$)

The amount of energy released in $\beta^- \beta^-$ decay is a fixed quantity, called the decay Q-value ($Q_{\beta\beta}$) and given by the mass difference between the parent and daughter nucleus, subtracted by the masses of the two emitted electrons:

$$Q_{\beta\beta} = M(A, Z) - M(A, Z + 2) - 2m_e \tag{6}$$

In the $2\nu\beta\beta$ decay mode, part of the energy is carried away by the anti-neutrinos and is essentially undetectable. As a result, the spectrum for the sum kinetic energy of the two electrons is continuous between 0 and $Q_{\beta\beta}$ (see Figure 1). In the $0\nu\beta\beta$ decay mode, neglecting the nuclear recoil, all the energy is carried by the electrons and is equal to the Q-value of the transition.

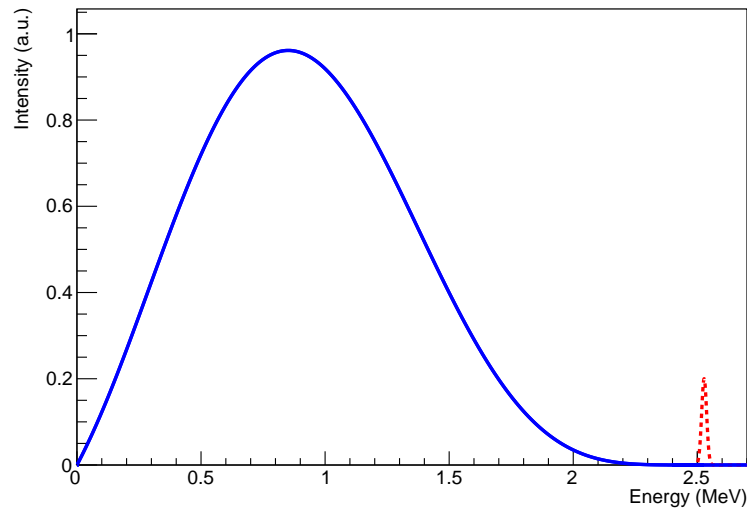


Figure 1. Schematic view of the combined energy spectrum of emitted electrons in ^{130}Te $2\nu\beta\beta$ (blue solid) [22] and $0\nu\beta\beta$ (red dashed) decay. The latter is modeled as a Gaussian of 10 keV standard deviation centered at $Q_{\beta\beta}$. The relative amplitude of the two spectra is arbitrary.

Therefore, the experimental signature of this process is very clear: if we consider the two electrons as a single body, we expect to observe a mono-energetic peak at $Q_{\beta\beta}$. Besides, the two emitted electrons point to the same interaction vertex. Most recent limits on the half life for several isotopes lie in the range of $\sim 10^{23}$ – 10^{26} yr [1].

2.2. Double Positron Decay ($\beta^+\beta^+$)

Neutrinoless double positron decay has a very distinctive signature: in addition to the two positrons, four annihilation 511-keV γ quanta will be detected if an event is observed. On the other hand, the rate for this process should be much lower in comparison with $0\nu\beta^-\beta^-$ decay for two reasons. The former is the substantially lower kinetic energy available in such a transition due to the presence of positrons in the final state. In fact,

$$Q_{\beta^+\beta^+} = M(A, Z) - M(A, Z - 2) - 4m_e \quad (7)$$

where M indicates the mass of the mother (daughter) atom. The latter motivation is the Coulomb repulsion on positrons from the nucleus. What distinguishes the $2\nu\beta\beta$ mode is that part of the energy is carried away by the emitted neutrinos and the combined kinetic energy of the positrons is again a continuous function between 0 and $Q_{\beta\beta}$.

Given the stringent energy requirement, there are only 6 candidates for this type of decay: ^{78}Kr , ^{96}Ru , ^{106}Cd , ^{124}Xe , ^{130}Ba and ^{136}Ce . In the interacting boson model [23], the half lives of the most promising isotopes are estimated to be $\sim 10^{27}$ – 10^{28} yr (for $\langle m_\nu \rangle = 1$ eV and $g_A = 1.269$). Compared to the $0\nu\beta^-\beta^-$ decay results presented above, this is approximately 10^3 – 10^4 times higher.

2.3. Positron Emitting Electron Capture ($EC\beta^+$)

Considering the $0\nu EC\beta^+$ mode, the signature is again quite clear: a positron and two annihilation 511-keV γ s are emitted. Furthermore, this process is not as strongly suppressed as $0\nu\beta^+\beta^+$. The available phase space is higher, and the total kinetic energy is:

$$T_{0\nu EC\beta^+} = M(A, Z) - M(A, Z - 2) - 2m_e - E_b \quad (8)$$

$$= Q_{EC\beta^+} - E_b \quad (9)$$

where M stands for atomic mass and we have taken into account the binding energy E_b of the captured electron. NME within the framework of the microscopic interacting

boson model (IBM-2) have been computed for the $\beta^+\beta^+$ candidates listed above, ^{58}Ni , and ^{64}Zn [24]. Combining these results with a calculation of the phase space factors [25], expected half lives can be extracted. In this case, half life estimates for the most promising nuclei give $\sim 10^{26}\text{--}10^{27}$ yr assuming $\langle m_\nu \rangle = 1$ eV and $g_A = 1.269$. ^{124}Xe is expected to have the shortest half life for $0\nu EC\beta^+$ decay [23].

If $0\nu\beta\beta$ decay is ever observed, it will be very important to clarify the underlying physics mechanism, and β^+EC modes show an enhanced sensitivity to right-handed weak currents, as is discussed in [26].

2.4. Double Electron Capture (ECEC)

A signature of the two-neutrino ECEC process in a direct experiment is the emission of two (or more) X-rays, which occurs following the capture of orbital electrons. The detectors used for these searches should therefore have good energy resolution and be sensitive to low energies. The observation of the two-neutrino mode of this decay is an important input to NME calculations, which can probe aspects of the models that are different from those addressed by the $\beta^-\beta^-$ decay.

From the experimental point of view, the first positive result was obtained in 2001 by a geochemical experiment with ^{130}Ba , where the SM-allowed double electron capture ($2\nu ECEC$) was detected with an half life of $T_{1/2}^{2\nu} = (2.2 \pm 0.5) \times 10^{21}$ yr [27]. Evidence of $2\nu ECEC$ in ^{78}Kr was then observed, as highlighted in [28]. A direct observation of double electron capture in ^{124}Xe was later possible with the XENON1T dark matter detector. The measured half life is $T_{1/2}^{2\nu} = (1.8 \pm 0.5 \text{ (stat.)} \pm 0.1 \text{ (syst.)}) \times 10^{22}$ yr [29].

Moving to the neutrinoless mode of this transition ($0\nu ECEC$), the available kinetic energy is higher, and Coulomb repulsion does not play a role. However, this decay mode is the most suppressed, since it must be accompanied by a radiation process in order to conserve energy, momentum and angular momentum. Details on this topic can be found in [30] and references presented therein. Even if the rate is practically independent of the decay energy and increases with higher Z , it is very low with half lives of $T_{1/2}^{0\nu} \sim 10^{28}\text{--}10^{31}$ yr [31].

However, the rate could be increased by $\sim 10^6$ times if resonance conditions exist, i.e., if the decay occurs into an excited state of the daughter, which is degenerate in energy with the initial state [30]. With this enhancement, the process starts to be competitive with $0\nu\beta^-\beta^-$ decay sensitivity to neutrino mass and it is possible to check this by experiment. There are several candidates for such resonance transitions, both to the ground and excited states of the daughter nuclei. Nonetheless, a precision well below 1 keV is required to realize such conditions. This possibility is discussed in [30,32]. The best present experimental limits are presented as well.

2.5. Double Beta Decay to the Excited States

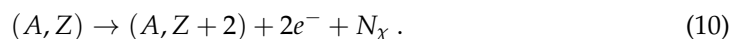
The $0\nu\beta\beta$ and $2\nu\beta\beta$ decays to excited states are interesting for different reasons. Theoretical calculations of the nuclear matrix elements for $2\nu\beta\beta$ use many-body techniques, nuclear models and approximations that can be generalized to $0\nu\beta\beta$ transitions. Many open issues exist on this topic [4,33], and validation of nuclear models via precise measurement of $2\nu\beta\beta$ half lives is crucial to resolve them and provide insight on nuclear dynamics [34]. In addition, the light Majorana neutrino exchange is not the only possible mechanism underlying $0\nu\beta\beta$ decay. The observation of multiple modes of the $0\nu\beta\beta$ transition, including decay on excited states, can disentangle the underlying mechanism [35].

Positive results of $2\nu\beta\beta$ decay searches to excited states exist to date just for 2 emitters. The involved nuclei are ^{100}Mo [36] and ^{150}Nd [37], with half lives of $(T_{1/2})_{0^+}^{2\nu} = 6.1_{-1.1}^{+1.8} \times 10^{20}$ yr and $(T_{1/2})_{0^+}^{2\nu} = 1.4_{-0.2}^{+0.4} \text{ (stat.)} \pm 0.3 \text{ (syst.)} \times 10^{20}$ yr, respectively. Lower limits exist for other $\beta\beta$ emitters ranging from 3.5×10^{18} yr to 8.3×10^{23} yr [38]. It is worth mentioning that all $\beta\beta$ emitters have a 0^+ ground state. When listing open channels for $\beta\beta$ decay to excited states, we must consider both the angular momentum of the final state and the available phase space. The higher the excitation level, the smaller the phase space, and correspondingly, the

decay rate. $0^+ \rightarrow 0^+$ transitions are favored over $0^+ \rightarrow 2^+$, while higher multiplicities are usually neglected due to the stronger suppression. The Te isotopes where $\beta\beta$ decay to excited states are allowed are ^{130}Te and ^{128}Te . We will discuss each of them individually.

2.6. Double Beta Decay with Majoron Emission

Besides $2\nu\beta\beta$ and $0\nu\beta\beta$, there is a third possible mechanism for double beta decay. In this case, one or more light neutral bosons χ (Majorons) are emitted:



The interest in this decay is mainly related to the existence of Majorons, massless Goldstone bosons that arise upon a spontaneous breakdown of a global B–L symmetry. They were postulated in various extensions of the standard electroweak theory [39]. Depending on their transformation properties under weak isospin, several models exist [13,39–41].

3. Experimental Techniques

The discovery potential of different experimental searches for double beta decay depends on few parameters that summarize the detector features and performance [42]. The probed physical observable is the decay half life $T_{1/2}$. The simplest case is a peak search such as $0\nu\beta\beta$ over a background, which we describe with a background index B representing the number of detected background events per unit energy, time and mass of $\beta\beta$ emitter. From the law of radioactive decay, we can derive:

$$T_{1/2} = \ln 2 t \epsilon \frac{N_0}{N} \quad (11)$$

where t refers to the live time, ϵ to the detection efficiency, N_0 and N are the number of emitter nuclei and decay events, respectively. Let Δ be the experimental energy resolution in the signal region, and consider as *signal window* an energy bin large Δ . The number of signal counts that corresponds to a detection, or rather to the expected upper limit the experiment can place in the case that no signal is present, is a (n_σ) multiple of the Poisson fluctuation of the number of background events detected in the signal window, according to the significance level the experiment sets. From these assumptions and Equation (11), the sensitivity assumes the following expression:

$$S_{1/2} = \ln 2 \epsilon \frac{1}{n_\sigma} \frac{x_e \eta_e N_A}{m_e} \sqrt{\frac{Mt}{B\Delta}} \quad (12)$$

where x_e is the stoichiometric multiplicity of the compound that contains the emitter, N_A is the Avogadro constant, η_e the isotopic abundance of the emitter in the source compound, m_e its molecular mass, and M its total mass. Despite being an approximate expression, Equation (12) highlights the role of the essential experimental parameters. The background level B , together with the maximum foreseen live time and the energy resolution Δ , can place an experiment beyond the validity boundaries of Equation (12). In fact, should the number of expected background events in the signal window be of order unity or smaller, it can be shown that the sensitivity has to be replaced by the background-free expression

$$S_{1/2} = \ln 2 \epsilon \frac{1}{n_\sigma} \frac{x_e \eta_e N_A}{m_e} Mt \quad (13)$$

This is a fortunate experimental condition sought by many next generation $0\nu\beta\beta$ experiments in that the sensitivity scales linearly with the exposure, i.e., the product of live time and source mass (Mt), and grows faster.

In the following, we outline the main experimental techniques, whereby double beta decay in tellurium isotopes is investigated.

3.1. Calorimeter-Tracking Experiments

A notable approach to $\beta\beta$ decay searches is given by calorimeter tracking experiments. They aim at excellent background rejection capabilities with a tracking detector able to identify the topology of $\beta\beta$ decays originating from a common vertex. The tracker is enclosed in a calorimeter to measure the kinetic energy of each track. This approach provides a unique tool to measure individual energy and angular distributions of the emitted electrons. A long history of such devices started in 1988 [43,44] and provided results on several $\beta\beta$ emitter nuclei with the NEMO-3 experiment [45] operated at the Modane Underground Laboratory. An upgraded version of this technique is foreseen in the future SuperNEMO experiment [46]. A SuperNEMO demonstrator is in a late commissioning phase [47], but investigation of Te isotopes is not planned. For this reason, we will focus just on the NEMO-3 experiment in the following.

The NEMO-3 experiment has a cylindrical structure, segmented into 20 sectors. This allows the deployment of thin source foils including different $\beta\beta$ emitter nuclei. The source foils have a diameter of 3.1 m, are 2.5 m tall and 30–60 mg/cm² thick. They are fixed vertically in between two concentric cylindrical tracking volumes. The tracking system is based on open Geiger drift cells. Plastic scintillator calorimeters are read out by low radioactivity photomultiplier tubes that surround the cylindrical volume. A 25 G coaxial magnetic field allows for particle and charge identification. The attained relative energy resolution at 1 MeV is 15% FWHM². The electron timing resolution is 250 ps.

The NEMO-3 experiment was primarily designed to search for $0\nu\beta\beta$ decay to the ground state, but included searches of $0\nu\beta\beta$ to the 2^+ excited state, $\beta\beta$ decay with Majoron emission ($\chi\beta\beta$) and $2\nu\beta\beta$ in a set of different isotopes. Backgrounds are split into three contributions: internal (due to the source foil), tracking volume, external. Internal backgrounds include long lived isotopes embedded in the source foil. Tracking volume backgrounds model contaminants in the tracking gas and in the drift cell wires. They are dominated by radon out of secular equilibrium and its daughters. External backgrounds originate from traces of ²¹⁴Bi, ⁴⁰K and ²⁰⁸Tl embedded in the PMT glass and electronics [48].

The NEMO-3 Collaboration set two main criteria to select candidate nuclei for $0\nu\beta\beta$ searches:

1. Transition energy $Q_{\beta\beta} > 2615$ keV so that most natural gamma backgrounds are suppressed;
2. Isotopic abundance $\eta > 2\%$ to ease the enrichment process and source production.

Furthermore, it was able to identify five nuclei that fulfilled both requirements: ¹¹⁶Cd, ⁸²Se, ¹⁰⁰Mo, ⁷⁶Zr and ¹⁵⁰Nd. The isotope of interest for this review, ¹³⁰Te, was added for a different reason, i.e., to study its $2\nu\beta\beta$ mode. Despite the below threshold $Q_{\beta\beta} \sim 2527$ keV, the experimental apparatus had a chance of settling controversial results from geochemical experiments (see Section 3.2). By the time the NEMO-3 detector was designed, there was only a measurement of the half life of ¹³⁰Te obtained with this technique. An exception is the first result from cryogenic calorimeters [49], which was not conclusive anyway. The NEMO-3 experiment housed both natural Te, which includes a 207 g component of ¹³⁰Te, and a (89.4 ± 0.5)% enriched sample including 454 g of ¹³⁰Te [48]. It collected 1257 days of live time, which correspond to a ¹³⁰Te exposure of ~ 2.3 kg·yr.

3.2. Geochemical Experiments

This indirect experimental technique is based on the determination of the presence of the double beta decay products in geological samples of known age, by evaluating the ratio of parent/daughter nuclei amounts. The measurements and limits extracted with this method are thus not sensitive to the $\beta\beta$ decay mode, and refer to the sum of all the possible ones ($2\nu\beta\beta$ or $0\nu\beta\beta$ to the ground state or to excited states).

The study of double beta decay half lives of tellurium isotopes takes advantage of geological telluride samples, that typically formed in hydrothermal vein-gold mineralization and whose age is determined with isotopic geochronometry methods [50]. The first results on the $\beta\beta$ decay half lives of several nuclei were obtained with these studies; for a long

time, until the first evidence of $2\nu\beta\beta$ decay of ^{130}Te was obtained with a direct experiment in 2003 [49], the only available knowledge on the $\beta\beta$ half lives of ^{128}Te and ^{130}Te came from geochemical experiments. The first measurement of $\beta\beta$ decay of ^{130}Te was obtained in 1950 by M. G. Inghram and J. H. Reynolds, who studied a 317 g sample of a Bi_2Te_3 crystal with age of 1.5 Gyr [51]. This was crushed and broken in smaller sizes, and then vacuum heated at temperatures above its melting point to obtain the mineral decomposition. The gas produced from the boiling bismuth and tellurium was then purified and analyzed in a 60° single-focusing mass spectrometer [52], and was found to be composed of argon and xenon. From the xenon isotopic analysis, an excess of ^{130}Xe was observed and it was attributed to $\beta\beta$ decay of ^{130}Te with an half life of 1.4×10^{21} yr.

Following this first result, several other analyses of telluride samples were performed with minerals of different ages, and two groups of ^{130}Te half lives measurements incompatible within the quoted uncertainties emerged [10,53–55] reported values in the range $T_{1/2} = (7.9\text{--}8.2) \times 10^{20}$ yr, while [56,57] obtained larger measurements such as $T_{1/2} = (2.5\text{--}2.7) \times 10^{21}$ yr. In particular, they noticed that experiments studying younger minerals (~ 100 Myr) obtained shorter half lives, while those using samples older than 1 Gyr reported longer values.

Subsequent studies suggested that the shorter half lives are more likely the correct ones (see [58] and references therein), and provided a possible explanation for the discrepancy between the results from young and old samples. When the half life value is computed in these studies, the complete retention of Xe daughter is assumed; however, its quantity in the geological sample could have been altered for several reasons over time. Post-formation geothermal episodes occurred more than 1 Gyr ago could be responsible for losses of xenon by thermal diffusion, and if this is the case, an overestimation of the half life can be obtained. On the contrary, an underestimation of the half life could result from younger samples if an additional quantity of ^{130}Xe accumulates in the analyzed mineral, e.g., inheriting it from older telluride formations or from the aqueous medium where they were created.

This controversy was later definitely solved thanks to the direct measurements of the $2\nu\beta\beta$ decay half life of ^{130}Te [48]. The average value obtained from the most recent experiments with young samples is given by [10]

$$T_{1/2} = (8.4 \pm 0.9) \times 10^{20} \text{ yr} \quad (14)$$

which is compatible with the most precise measurement currently available [59].

3.3. Cryogenic Calorimeters

Cryogenic calorimetry is an approach to rare event searches that leverages phonon detection to measure the energy released by particle interactions in the detector material. It is very widely employed, besides the search for $0\nu\beta\beta$ decay, in dark matter detectors, X-ray astronomy and astrophysics and other fields [60]. Cryogenic calorimeters are usually operated at a few tens of mK and they rely on the small heat capacity of the absorber at such low temperatures. To achieve low enough heat capacities, the choice of materials must be restricted to dielectric and diamagnetic ones, or superconductors below their transition temperature so that the heat capacity follows the Debye law. Energy releases in the absorber yield a temperature increase, that can be detected with phonon sensors and turned into an electric signal. Despite being insensitive to particle directionality, cryogenic calorimeters can achieve a very good energy resolution, which was pushed at the level of a few 10^{-3} at the reaction Q-value [61–64].

A substantial development of this technique was based on TeO_2 thermal detector crystals (see [65] and references therein). The CUORE experiment [66,67], which is located at the Laboratori Nazionali del Gran Sasso (LNGS) in Italy, is the culmination of this long effort and is the only currently running tonne-scale array of such devices. Its smaller scale predecessors, CUORE-0 [68] and CUORICINO [69], contributed to improving knowledge in the $\beta\beta$ decay channels of several Te isotopes, with a collected ^{130}Te exposure of 9.8 kg·yr and 19.75 kg·yr, respectively. CUORE has recently released results based on 1038.4 kg·yr of

natural TeO_2 exposure [70], and was designed to collect 5 yr of live time, corresponding to ~ 3.6 tonne yr of raw exposure. The foreseen upgrade of CUORE will be based on scintillating Li_2MoO_4 bolometer crystals instead, in order to provide background rejection capabilities via dual readout of the heat and light signal aiming at a background-free regime [71]. For this reason, we will not discuss it further.

The CUORE detector is an array of 988 natural TeO_2 crystals, arranged in a cylindrical structure of 19 towers. Each tower has 13 floors of 4 crystals each, held together by a copper frame. The compact geometrical arrangement of the CUORE detector is such that self-shielding reduces the γ background in the inner detectors and a coincidence analysis acts both as a veto for background events and as a good tag for decay modes where multiple secondaries are emitted.

Its 90% Bayesian Credibility Interval (C.I.) limit setting sensitivity to $0\nu\beta\beta$ decay after 5 yr of live time is expected to be $\sim 5.3 \times 10^{25}$ yr if we scale the one quoted in [70] by a factor given by the square root of the exposure ratio according to Equation (12). Slightly different values are reported in [72], where a background index of $\sim 10^{-2}$ counts/(keV kg yr) was used and yielded a 90% C.I. limit setting sensitivity of $(6.1\text{--}8.9) \times 10^{25}$ yr assuming a 5 keV (upper bound) and 10 keV (lower bound) resolution. CUORE lies in between in terms of resolution, but observed a 50% higher background than the one assumed in [72]. Even though CUORE was designed with the main goal of searching for $0\nu\beta\beta$ decay of ^{130}Te , its crystals made of natural Te will provide an extremely large exposure of ^{128}Te (isotopic abundance $\eta_{128} \sim 32\%$). In addition, besides their small isotopic abundance of $\eta_{123} \sim 0.9\%$ and $\eta_{120} \sim 0.1\%$, a remarkable exposure will be accumulated for the other very long lived isotopes of Te, making the analysis of the CUORE data an opportunity to improve many of the results that we review here.

3.4. Liquid Scintillator-Based Experiments

Experiments of this kind measure the radioactivity of a sample by mixing the active material with a liquid scintillator (LS): the energy released produces the emission of photons whose signal is detected with photomultipliers. There are typically two components in LS: solvents that form the bulk, and fluors with an emission spectrum that matches the response of the photodetectors as a dopant. Both the KamLAND-Zen (^{136}Xe) [73] and SNO+ (^{130}Te) $0\nu\beta\beta$ experiments use PPO (2,5-diphenyloxazole) as fluor. Although liquid scintillators do not have superior energy resolution, their main appeal as $0\nu\beta\beta$ decay detectors is the mass scalability. Unlike other $0\nu\beta\beta$ experiments with solid state targets, contaminants in the liquid scintillator (LS) may be removed online. Moreover, the $0\nu\beta\beta$ emitter concentration can be varied during operations. This allows systematic checks of rate scaling in the event of a discovery, as well as background stability as a function of the concentration of the source material.

The SNO+ experiment [74] is the direct successor to the Sudbury Neutrino Observatory (SNO), which had a primary role in the discovery of neutrino flavor oscillations [75]. It is a large multipurpose neutrino detector located 2 km underground at SNOLAB, Sudbury, Canada. The muon flux is ~ 63 events per day in a 8.3-m radius circular area [76].

The main detector is a 6-m radius acrylic vessel (AV), to be filled with 780 tonnes of linear alkylbenzene (LAB) as a solvent and PPO as fluor (the concentration is 2 g/L). LAB was selected based on several factors, mainly the possibility to dissolve heavy metals with long term stability and good optical properties. Furthermore, as far as timing is concerned, results presented in [77] show that $>99.9\%$ alpha particles are rejected while keeping $>99.9\%$ of electrons. To shift the emission peak to roughly 390–430 nm and better match the PMT quantum efficiency 1,4-Bis (2-methylstyryl) benzene (bis-MSB) (15 mg/L) will be added to the mixture.

Neutrino interactions within the AV are viewed by ~ 9300 PMTs, whereas ~ 90 outward facing PMTs are used to tag cosmic rays. The PMT support structure is located in a ~ 18 -m cavity filled with ~ 7000 tonnes of ultra-pure water (UPW) that behaves as an active shield from radioactivity. The detector calibration systems include both optical sources to verify

the PMTs and radioactive sources (see [74] for a complete list) to check the energy scale and the energy resolution in a wide range from 0.1 to 6 MeV.

The primary goal of SNO+ is the search for $0\nu\beta\beta$ decay of ^{130}Te . Its potential to explore other physics such as reactor $\bar{\nu}$ oscillations and solar neutrinos is described in [74]. The liquid scintillator will initially be loaded with 0.5% natural Te by mass (~ 1300 kg). An organo-metallic compound of telluric acid and butanediol (TeBD) is formed and directly mixed into the liquid scintillator. A stabilizer called Dimethyldodecylamine (DDA) will be added to increase the light yield and improve the stability against water. This loading technique is highly scalable in LS and has a relative low cost ($\lesssim \$2$ M per tonne of $0\nu\beta\beta$ isotope). Furthermore, it allows optical transparency to be preserved: the total expected light yield is ~ 460 pe/MeV.

The SNO+ collaboration is almost ready to start tellurium loading in a liquid scintillator (Phase I). During the previous one, the AV was filled with 905 tonnes of UPW and a few months of data were acquired to compare external backgrounds with expectations. Moreover, new limits on specific channels of invisible nucleon decays were set, and the ^8B solar neutrino flux was measured and confirmed to be compatible with previous results [78].

Among other reasons, ^{130}Te has been selected for its high natural isotopic abundance ($\sim 34\%$) and because the $2\nu\beta\beta$ half life is one of the largest among $0\nu\beta\beta$ emitters: energy resolution is a limiting factor for SNO+ (some hundreds of keV).

An asymmetric region of interest (ROI) from -0.5σ (2.49 MeV) to 1.5σ (2.65 MeV) around the signal peak will be considered [79]. Internal (inside the AV) and external background levels can be measured before and after the isotope deployment, allowing identification and removal of possible contamination. This is true for the detector response as well, since it can be tested with or without tellurium in the scintillator cocktail. Most of external background contributions are rejected with a 3.3-m fiducial radius cut, while preserving 20% of signal events. The main background sources falling inside the fiducial volume and the $0\nu\beta\beta$ ROI are elastically scattered electrons from ^8B solar neutrinos, the internal ^{232}Th chain, external γ s, $2\nu\beta\beta$ events, the internal ^{238}U chain, cosmogenic background, (α, n) reactions and pile-up events [74]. They are ordered according to the expected event rate in the ROI. Given previous measurements from other experiments, i.e., Borexino (^8B solar neutrinos) and CUORE ($2\nu\beta\beta$), and the initial water phase, an estimate of about ten events in the ROI was extracted [79]. The Te-loaded scintillator purity level aimed for the ^{238}U (^{232}Th) chain is 2.5×10^{-15} g/g (2.8×10^{-16} g/g). Background rejection techniques are mostly based on the analysis of delayed coincidences and PMT timing distribution [74].

The projected sensitivity on ^{130}Te $0\nu\beta\beta$ half life after five years of data taking is $T_{1/2}^{0\nu} > 1.9 \times 10^{26}$ yr (90% C.L.), that corresponds to a limit on the effective Majorana mass of 41–99 meV, with range defined by the nuclear matrix element calculations [79]. An increase in tellurium loading from 0.5% to 2.5% in phase II could achieve a limit setting sensitivity of $T_{1/2}^{0\nu} \sim 10^{27}$ yr.

3.5. Semiconductor Detectors

Semiconductor detectors measure the energy released by impinging particles integrating the drift current of electron-hole pairs produced by ionizing radiation in a charge depleted volume. In order to reduce thermal generation of electron-hole pairs, semiconductor detectors need often to be operated at low temperatures, but that strongly depends on the energy gap between conduction and valence band. The number of excitations is proportional to the energy released in the detector. A notable application of semiconductor detectors to $\beta\beta$ decay searches is high-purity Ge detectors (HPGe), both as general tools to perform gamma spectroscopy [80] and, since ^{76}Ge is a $\beta\beta$ emitter, in a source = detector approach [81].

A multi-purpose semiconductor experiment based on CdZnTe detectors was proposed by the COBRA Collaboration [82]. It naturally includes nine $\beta\beta$ emitter nuclei, among which Te, but its main focus is on ^{116}Cd . It has the great advantage that can be operated at

room temperature as opposed to HPGe detectors. A demonstrator is currently running at the LNGS in Italy, but a significant improvement in the deployed mass is foreseen in order to start exploring the inverted hierarchy region of neutrino masses [83].

4. ^{130}Te

4.1. Standard Model Decay Mode: Half Life Measurement

To date, the only observed decay mode of ^{130}Te is $2\nu\beta\beta$ to the ground state of ^{130}Xe . First measurements were performed on geological samples and provided controversial results (see Section 3.2). The direct measurement from the NEMO-3 collaboration (see Section 3.1) finally solved the controversy [48], setting the half life to

$$T_{1/2}^{2\nu} = (7.0 \pm 0.9_{\text{stat}} \pm 1.1_{\text{syst}}) \times 10^{20} \text{ yr} \quad (15)$$

The latest and most precise measurement of the half life to date comes from the cryogenic bolometers of the CUORE experiment [59], which is in agreement with the first direct detection result

$$T_{1/2}^{2\nu} = 7.71_{-0.06}^{+0.08}(\text{stat.})_{-0.15}^{+0.12}(\text{syst.}) \times 10^{20} \text{ yr} \quad (16)$$

A question of great theoretical interest that precision measurements of $2\nu\beta\beta$ decay can address is whether the spectrum better fits the single state (SSD) or higher state dominance (HSD) hypotheses. Both models relate to the Gamow-Teller (GT) nuclear matrix element component. The former considers the GT term derived from the lowest energy virtual intermediate 1^+ state to be the dominant contribution to the overall result. The alternate HSD hypothesis assumes the dominant part to the $2\nu\beta\beta$ rate is due to higher order states of the intermediate nucleus. In the SSD hypothesis the factorization of the nuclear part from the integration over phase space is exact. Conversely, in the HSD hypothesis in order to separate the PSF and the NME, closure approximation is needed [84–86]. To date, a slight preference for SSD in ^{130}Te was found [59], but the alternate hypothesis could not be completely excluded.

4.2. Beyond Standard Model Decay of ^{130}Te

In this section, we will describe the ^{130}Te $0\nu\beta\beta$ decay focusing on the leading mechanism, i.e., the transition to the ground state of ^{130}Xe . As it was mentioned earlier, the first approach adopted to investigate $\beta\beta$ decay in ^{130}Te was based on geochemical measurements [58], that were not able to distinguish between the 2ν and the 0ν mode. Later in the 1980s, a measurement with a scintillator-based experiment was performed to study lepton number violation and set a new limit on ^{130}Te half life for $0\nu\beta\beta$ [87]. In 2011, the NEMO-3 experiment investigated such decay, providing a limit of $>1.3 \times 10^{23}$ yr at 90% Confidence Level (C.L.) [48]. At present, liquid scintillators (SNO^+ [74]) and solid state detectors (CUORE [67], COBRA [83]) are employed to study ^{130}Te $0\nu\beta\beta$ decay. However, the most powerful technique for this analysis remains the use of TeO_2 thermal detectors. Since SNO^+ data taking has not started yet and COBRA is in a preliminary phase, from now on we will focus on the results obtained with cryogenic calorimeters. We try to highlight the major improvements introduced throughout the years.

The first result was a lower limit of 2.7×10^{21} yr extracted from a 73.1 g TeO_2 detector [88]. This was enough to surpass the most stringent constraint at the time, i.e., $T_{1/2}^{0\nu} > 2.6 \times 10^{21}$ yr, that was obtained with the geochemical technique [89]. The following step was the successful operation of a $3 \times 3 \times 6$ cm³ TeO_2 crystal of 334 g of mass [90], that became the unitary element of the first bolometric array with large-mass crystals. It was MiDBD (Milan Double Beta Decay), a solid state detector made of 20 bolometers (five floors of four crystals each), for a total TeO_2 mass of 6.8 kg. MiDBD achieved an energy resolution of 5 keV at $Q_{\beta\beta}$ and a very low background of <1 counts/(keV·kg·yr) in the Region of Interest (ROI). In 2002, with an accumulated exposure of 4.25 kg·yr, MiDBD was

able to set a limit of $T_{1/2}^{0\nu} > 2.1 \times 10^{23}$ yr at 90% C.L. on the lepton number violating decay of ^{130}Te .

Furthermore, MiDBD set a limit on the half life of $0\nu\beta\beta$ with Majoron emission³ of $T_{1/2}^{\chi} > 2.2 \times 10^{21}$ yr as well, which was not updated by subsequent cryogenic calorimeter experiments [49]. A more stringent limit was set by the NEMO-3 Collaboration as $T_{1/2}^{\chi} > 1.6 \times 10^{22}$ yr (90% C.L.) [48]. It corresponds to a limit of $g_{ee} < (0.6\text{--}1.6) \times 10^{-4}$ on the neutrino–Majoron coupling constant. Current limits on the neutrino–Majoron coupling constant from $0\nu\beta\beta$ experiments are of the order of $\sim 10^{-5}$ [7].

In parallel with the operation of MiDBD, a massive production of high quality TeO_2 crystals began [91] and the idea of building a bolometer array with 1000 cryogenic detectors, i.e., CUORE, gained a foothold. Cuoricino was designed as a proof of concept for CUORE: its detector was made of a single tower with a total TeO_2 mass of 40.7 kg. By collecting a ^{130}Te exposure of 19.75 kg·yr, Cuoricino demonstrated the feasibility of running a bolometric detector array for almost five years. It also provided relevant physics results on its own, setting a lower bound on the ^{130}Te $0\nu\beta\beta$ half life of $T_{1/2}^{0\nu} > 2.8 \times 10^{24}$ yr [69], surpassing by an order of magnitude the sensitivity of NEMO-3 that was running at the same time. Among the two subsets employed, the best performance in terms of background counts and resolution was obtained with $5 \times 5 \times 5$ cm³ crystals made of natural Te. The harmonic mean resolution at the 2615 keV ^{208}Tl line was (5.8 ± 2.1) keV (FWHM), whereas the background index in the region of interest was (0.153 ± 0.006) counts/(keV·kg·yr) [92].

During the Cuoricino data taking, a big effort was devoted to the study of background sources in view of the forthcoming CUORE. It was known that the main contribution was due to degraded α s from either the crystal surfaces or the support structure parts. A new design for the detector structure was proposed to minimize the amount of copper facing the TeO_2 crystals and a new production and treatment protocol for CUORE crystals was validated [93]. Furthermore, an automated procedure for copper cleaning and detector assembly was introduced [94,95].

The final test for CUORE consisted of operating as a standalone experiment a prototype tower, CUORE-0. It was comprised of a single tower, with 52 5-cm size cubic crystals made of ^{nat}Te and arranged in 13 floors of 4 crystals each. The total mass of TeO_2 was 39 kg [92]. The detector was housed in the same cryostat as Cuoricino and collected data from 2013 to 2015. The harmonic mean resolution at the 2615 keV ^{208}Tl line was measured to be (4.9 ± 2.1) keV. There was a factor 7 improvement in the α background rejection compared to Cuoricino, and a factor 3 improvement in the ROI background, as the measured background index was $(0.058 \pm 0.004(\text{stat.}) \pm 0.002(\text{syst.}))$ counts/(keV·kg·yr). Finally, with an accumulated ^{130}Te exposure of 9.8 kg·yr, a lower limit on the ^{130}Te $0\nu\beta\beta$ half life of $T_{1/2}^{0\nu} > 2.7 \times 10^{24}$ yr was set. Combining this result with the measurement from Cuoricino, a lower bound of $T_{1/2}^{0\nu} > 4.0 \times 10^{24}$ yr was established [68,96].

CUORE commissioning ended in 2016, and data taking began in 2017. Its detector is a close-packed array of 988 TeO_2 bolometers arranged in a cylindrical matrix of 19 identical towers. The total TeO_2 mass is 742 kg, corresponding to ~ 206 kg of ^{130}Te . CUORE is by far the largest detector operated as a bolometer. In these years, there have been three data releases with TeO_2 exposures of 86.3 [97], 372.5 [61] and 1038.4 kg·yr [70], respectively. The measured energy resolution at $Q_{\beta\beta}$ is (7.8 ± 0.5) keV, slightly worse than expected from CUORE-0. The background index in the ROI is $(1.49 \pm 0.04) \times 10^{-2}$ counts/(keV·kg·yr) in line with the experiment goal and mostly due to surface α contamination. The analysis of over 1 tonne-year exposure confirmed the absence of a signal of $0\nu\beta\beta$ decay and led to a lower limit of $T_{1/2}^{0\nu} > 2.2 \times 10^{25}$ yr at the 90% C.I [70]. The median exclusion sensitivity extracted from this search is 2.8×10^{25} yr. The data analysis procedure is described in detail in [70] and mostly follows the strategy adopted for CUORE-0 [96]. Recent improvements include a significant lowering of the detectors energy threshold thanks to the application of the optimum trigger algorithm based on the matched filter technique [98,99] and the introduction of a new methodology for pulse shape analysis with higher efficiencies [100]. The energy thresholds have a relevant role on the effectiveness of the anti-coincidence

analysis. CUORE perspective is to continue data taking until a total live time of 5 yr will be reached. Given the latest result, the projected limit setting sensitivity is approximately $S_{0\nu} = 5.3 \times 10^{25}$ yr. Several studies of noise sources and mitigation techniques are currently ongoing in order to improve detector performance over the next years, both for CUORE and in view of its future upgrade, i.e., CUPID [71].

4.3. ^{130}Te Decay to Excited States

Double beta decay to the excited states is suppressed with respect to the ground state. Energetic and angular momentum considerations imply that final states other than the lowest 0^+ and 2^+ states of the daughter nucleus are even more suppressed and can be safely neglected.

The most recent result on $0\nu\beta\beta$ decay of ^{130}Te in the $0^+ \rightarrow 2^+$ channel comes from bolometric experiments [49] that yielded a lower limit on the corresponding half life of

$$T_{1/2} > 1.4 \times 10^{23} \text{yr (90\%C.L.)}. \tag{17}$$

The available $\beta\beta$ decay study of ^{130}Te in the $0^+ \rightarrow 2^+$ transition performed in [101] with a Ge detector cannot discriminate the 0ν from the 2ν channel, since it is only sensitive to the de-excitation γ of the daughter nucleus. A limit on the lifetime of $\tau_{130} > 4.5 \times 10^{21}$ (68% C.L.) is reported.

A combination of the results from the CUORICINO [102] and CUORE-0 [103] data yields the strongest limits on the $0\nu\beta\beta$ and $2\nu\beta\beta$ decay to 0^+ excited states half-life of ^{130}Te , respectively,

$$(T_{1/2})_{0^+}^{0\nu} > 1.4 \times 10^{24} \text{ yr (90\% C.L.)} \tag{18a}$$

$$(T_{1/2})_{0^+}^{2\nu} > 2.5 \times 10^{23} \text{ yr (90\% C.L.)} \tag{18b}$$

Latest results from the CUORE experiment [104] push these limits even further as

$$(T_{1/2})_{0^+}^{0\nu} > 5.9 \times 10^{24} \text{ yr (90\% C.I.)} \tag{19a}$$

$$(T_{1/2})_{0^+}^{2\nu} > 1.3 \times 10^{24} \text{ yr (90\% C.I.)} \tag{19b}$$

It is useful to compare present results to the available theoretical calculations of the $2\nu\beta\beta$ channels. The expected theoretical $2\nu\beta\beta$ decay rate in different final states are given in terms of nuclear matrix element and phase space calculation results [22,33,34]. The ones based on the Quasi-particle Random Phase Approximation (QRPA) approach favor the following range [33]

$${}^{th}(T_{1/2})_{0^+}^{2\nu} = (7.2 - 16) \times 10^{24} \text{ yr} \tag{20}$$

We provide a range, rather than a single number, based on different phenomenological choices of quenching models for the effective axial coupling constant g_A . The lower bound assumes a constant function of the mass number A , the upper bound assumes a value of $g_A = 0.6$ [6,33,105].

An independent calculation of the ^{130}Te $2\nu\beta\beta$ decay rate to the first 0^+ excited state of ^{130}Xe within the IBM-2 framework based on [22,106] is reported in [34] as

$${}^{th}(T_{1/2})_{0^+}^{2\nu} = 2.2 \times 10^{25} \text{ yr.} \tag{21}$$

This calculation uses the ratio of phase space factors and nuclear matrix elements from the first excited and ground 0^+ states to compute the decay rate ratio for the two processes. Then, it exploits the measured rate of $2\nu\beta\beta$ to the ground state mode to derive Equation (21). The disagreement between Equations (20) and (21) is not an isolated case. In general, IBM-2 predictions disagree with the ones from QRPA, and for the nuclei where a $2\nu\beta\beta$ transition to excited states was observed, the measured half life is smaller than the predicted value.

On the contrary, examples exist where recent experimental limits on the half life rules out the QRPA prediction [34]. Moreover, the experimental $2\nu\beta\beta$ half life in the gs–gs transition quoted in [34,107] is a combination of results from geochemical experiments and direct detection with tracking calorimeters and bolometric experiments, which dates back to more than 10 years ago. The latest and more precise direct measurement of the ^{130}Te half life [59], entirely due to the $2\nu\beta\beta$ decay to the ground state of the daughter nucleus, is $\sim 13\%$ higher than the result used in [34]. This points to an even larger discrepancy between IBM-2 and QRPA predictions. For this reason, we believe it is important that experimental efforts further proceed to push the discovery sensitivity of $2\nu\beta\beta$ to excited states past the 2×10^{25} yr threshold. This is about one order of magnitude beyond the current limit setting sensitivity. An effort towards both data collection and refinement of the analysis techniques is required.

5. ^{128}Te

5.1. Standard Model Allowed Decay

To date, no direct observation of $2\nu\beta\beta$ decay of ^{128}Te was detected by counting experiments, due to the limitation given by the high background in the low energy range where this signal is expected. The transition energy of $Q_{\beta\beta} = (866.7 \pm 0.7)$ keV [108] lies in a highly populated region, dominated by the ^{130}Te $2\nu\beta\beta$ decay events and, secondarily, by the natural γ background due to environmental radioactivity. The only available knowledge on the half life of this SM-allowed decay of ^{128}Te comes from the geochemical approach.

The ^{128}Te double beta decay half life reported by geochemical experiments is usually determined from the ^{130}Te and ^{128}Te half lives ratio, which was precisely determined with ion-counting mass spectrometry of xenon in ancient tellurium samples [57]:

$$R = \frac{T_{1/2}(^{130}\text{Te})}{T_{1/2}(^{128}\text{Te})} = (3.52 \pm 0.11) \cdot 10^{-4} \quad (22)$$

From this ratio and the measured value of ^{130}Te double beta decay half life, the ^{128}Te one is extracted. The latest recommended value is obtained by exploiting the weighted average of the ^{130}Te half lives reported in [109,110], and from the half lives ratio one obtains [10]:

$$T_{1/2} = (2.25 \pm 0.09) \times 10^{24} \text{ yr} \quad (23)$$

As previously mentioned, the half life measurement obtained with the geochemical approach cannot distinguish among the decay modes and refers to the sum of all the possible ones, and since the $2\nu\beta\beta$ decay is the one with a higher expected rate, this can be considered as a measurement of the half life of this transition.

Among the experiments of current generation searching for double beta decay in tellurium isotopes, CUORE operates a total mass of 742 kg of natural TeO_2 crystals. Given the high isotopic abundance of ^{128}Te ($\sim 32\%$), this mass corresponds to 188.5 kg of the ^{128}Te isotope in the CUORE detector. Assuming the value in Equation (23) for the ^{128}Te $2\nu\beta\beta$ decay half life, ~ 275 counts are expected from this transition each 1 yr of live time. A future analysis in CUORE aims at a possible direct detection of this decay.

As for ^{130}Te decay to excited states, a study performed with a coaxial Ge(Li) detector surrounded with a layer of pure tellurium indicated a limit on the lifetime of the $0^+ \rightarrow 2^+$ transition of $\tau_{128} > 4.7 \times 10^{21}$ yr (68% C.L.) [101].

5.2. Beyond Standard Model Transition

Among the various isotopes under investigation, the study of the $0\nu\beta\beta$ decay of ^{128}Te is particularly interesting from the theoretical point of view since it can provide a discriminator among the different models that try to describe the mechanism underlying the phenomenon. Indeed, the ratio between the half lives of different isotopes can be used to compare theoretical predictions, and information can be gathered even in presence of an upper limit [111]. From the experimental point of view, the high natural abundance

of $\sim 32\%$ also makes this isotope an interesting candidate for the study of $0\nu\beta\beta$ decay. However, past direct search experiments used tens of kg of TeO_2 were characterized by a poor sensitivity to this process since, as mentioned in the above section, the signal peak at $Q_{\beta\beta} = (866.7 \pm 0.7)$ keV lies in a high background region of the spectrum. The most recent limit of [49]

$$T_{1/2}^{0\nu} > 1.1 \times 10^{23} \text{ yr (90\% C.L.)} \quad (24)$$

was obtained in 2003 by the MiDBD experiment, by means of the bolometric technique. MiDBD operated an array of 20 TeO_2 cryogenic crystals with two enriched in ^{128}Te at 82.3%, corresponding to a total mass of 6.8 kg in TeO_2 . This currently represents the most stringent limit on the half life of the $0\nu\beta\beta$ decay of this isotope, but it is not competitive with the result obtained from geochemical experiments reported in Equation (23): as this refers to the sum of all the possible decay modes, it can be considered as lower limit on the ^{128}Te $0\nu\beta\beta$ half life.

A significant improvement in the achievable sensitivity to this phenomenon is expected from direct search ton-scale experiments. CUORE is currently operating with 742 kg of TeO_2 , that corresponds to a factor ~ 100 higher mass with respect to the MiDBD detectors. According to the sensitivity expression reported in Equation (12), this corresponds to a ~ 10 times higher sensitivity expected from CUORE to this decay. CUORE can thus obtain limits competitive with the geochemical ones, and it might also be the first direct experiment even overcoming the geochemical measurement.

6. ^{123}Te

The ^{123}Te is a naturally occurring tellurium isotope with an isotopic abundance of $(0.8854 \pm 0.0006\%)$ keV [112]. The only kinematically allowed decay mode for this nucleus is a second-forbidden electron capture to the ground state of ^{123}Sb with a transition energy of $Q = (51.91 \pm 0.07)$ keV [108].

No clear evidence of this decay has been observed so far; theoretical calculations predict very low rates for this process due to a strong suppression of the nuclear matrix elements (see [113] and references therein). It was shown that the K shell capture is suppressed, and that the EC is most probably expected to occur from the L₃ shell [114,115].

Several experiments investigated this transition in the past and reported conflicting results. The first observation of ^{123}Te EC from K shell was claimed in 1962 by Watt and Glover [116], who indicated an half life of $(1.24 \pm 0.10) \times 10^{13}$ yr for this process using a proportional counter. With this experimental technique, the expected signal for this decay corresponds to the energy of the single X-rays from K shell of ^{123}Sb , that is 26.1 keV. This measurement, however, resulted to be in contrast with previous more stringent limits and was successively attributed to the X-ray emission from the K shell of Te atoms at 27.3 keV, which could not be distinguished from the expected signal due to a poor energy resolution.

A second evidence for ^{123}Te EC from K shell was claimed in 1996 with the use of cryogenic TeO_2 crystals operated as pure calorimeters, and a lifetime of $(2.4 \pm 0.9) \times 10^{19}$ yr was indicated [117]. In this case, the detector is also the source of the decay, thus the expected signal is given by the total binding energy of the captured electron, which is equal to 30.5 keV for the K shell. However, the same group later explained this observation with EC of ^{121}Te , and set a 90% C.L. lower limit of $T_{1/2}^{\text{K}} > 5 \times 10^{19}$ yr for the ^{123}Te EC from K shell; if the corresponding predicted branching ratio (1.83×10^{-3}) is accounted for, an inclusive limit of $T_{1/2} > 9.2 \times 10^{16}$ yr is obtained for EC of ^{123}Te [113]. Technological improvements in TeO_2 detectors allowed to achieve lower energy thresholds in the following years, and also the region of the spectrum where the signal of ^{123}Te EC from L shell became accessible: a line at ~ 4.7 keV and one at ~ 4.1 keV are expected in case of EC from L1 shell and from the most probable L3 shell, respectively. A line compatible with ^{123}Te EC from L1 shell has been observed [114], but its origin is still unclear.

The question of the existence of ^{123}Te EC decay is still open; the most promising experimental approach to investigate it turned out to be the calorimetric one, since it provides an excellent energy resolution and a detection efficiency that is close to 100%.

The CUORE experiment, with its ton-scale array of TeO₂ crystals and low background, is expected to achieve higher sensitivities to this rare decay: its granularity can be exploited to further reduce the background inducing energy releases in more than one crystal. A ¹²³Te EC decay is indeed expected to produce a signal in a single detector. If a signal was observed or even more stringent limits could be set, CUORE could possibly contribute to clarify the question of ¹²³Te EC decay.

7. ¹²⁰Te

Double beta decay of ¹²⁰Te can occur via β^+EC and double electron capture, both mechanisms have been investigated in the last twenty years. The first experimental limits were set using arrays of CdZnTe semiconductor detectors located at the Laboratori Nazionali del Gran Sasso [118–120] and a HPGe detector at the Modane Underground Laboratory [80], respectively.

With the former, the most recent result is based on a total CdZnTe exposure of 18 kg·days whereby a limit on ¹²⁰Te half life for $0\nu EC\beta^+$ transition was established: $T_{1/2}^{0\nu} > 4.1 \times 10^{17}$ yr (90% C.L.) [118]. The latter set a limit on the $(0\nu + 2\nu)\beta^+EC$ transition to the ground state of ¹²⁰Sn of $T_{0\nu+2\nu} > 1.9 \times 10^{17}$ yr (90% C.L.) [80].

Double electron capture (ECEC) was investigated as well and limits on $0\nu ECEC$ both to the ground state and to the first excited state ($E = 1171.3$ keV) of ¹²⁰Sn were extracted.

CdZnTe detectors set them to 2.4×10^{16} yr and 1.8×10^{16} yr, respectively, [118]. The $\beta\beta$ decay analysis with HPGe detector consisted of the search for γ -ray lines corresponding to the various decay schemes. The $0\nu ECEC$ transition to the ground state was studied considering three possible capture cases:

- 2 electrons from the *L* shell, in this case $E_b = 4.15$ keV is assumed since $E_L(2s)$, $E_L(2p1/2)$ and $E_L(2p3/2)$ (4.46, 4.15 and 3.393 keV, respectively) could not be resolved;
- 2 electrons from the *K* shell, this means that $E_b = 29.2$ keV;
- 1 electron from the *L* shell, the remaining one from *K* shell.

The extracted limits at the 90% C.L. lie between 1.9 and 6×10^{18} yr. Double electron capture to the first 2^+ excited state of ¹²⁰Sn was also considered, and a limit of 7.5×10^{17} yr on $T^{(0\nu+2\nu)}$ was obtained [80].

Afterwards, the Cuoricino experiment performed a search for the $EC\beta^+$ decay, considering both the 0ν and the 2ν mode. Double electron capture was not investigated since the maximum amount of energy released is ~ 60 keV and the detector thresholds were optimized for higher energies. With a total ¹²⁰Te exposure of 0.0573 kg·yr, a 90% C.L. limit on the ¹²⁰Te double beta decay half life was obtained: $T_{1/2}^{0\nu} > 1.9 \times 10^{21}$ yr for the neutrinoless mode and $T_{1/2}^{2\nu} > 7.6 \times 10^{21}$ yr for the 2ν mode, respectively, [121]. Compared to previous results, an improvement by almost three (four) orders of magnitude was obtained for the 2ν (0ν) mode. This analysis was performed under the following assumptions:

- Electron capture from the *K*-shell only (the ratio of *L*-capture to *K*-capture is ~ 10 % for most elements);
- The bolometer where the decay occurs will see the deposition of both the kinetic energy of the emitted positron and the binding energy E_b for a maximum energy of $T_{0\nu EC\beta^+} + E_b = 692.8$ keV (see Equation (8) and Table 1);
- The 511 keV photons resulting from the β^+ annihilation can either escape the detector or be absorbed in the same/a neighbor crystal and be detected as coincident events on multiple bolometers.

As a result a β^+EC event can produce six different scenarios, listed in Table 2.

Table 1. The most stringent results on known decay modes of Te isotopes are listed below. Positive results are quoted as central value, statistical and systematical uncertainty, in this order. Regarding ^{120}Te double electron capture decay, the available energy depends on the specific shells involved: the binding energy is 29.2 keV for the K shell, 4.46, 4.15 and 3.93 keV for the L shell. For the 0ν mode to the ground state, we report a range of half life limits, resulting from the possible combinations of the shells considered in [80]: K^1K^2, K^1L^2 and L^1L^2 . For the decay to the first excited state of ^{120}Sn we indicate the energy of the detected gamma-ray.

Isotope	Natural Abundance [%]	Decay Mode	Q-Value [keV]	$T_{1/2}$ [yr]	Ref.
^{130}Te	34.1668(16)	$2\nu\beta^-\beta^-$ (g.s.)	2527.515(13)	$7.71_{-0.06}^{+0.08}(\text{stat.})_{-0.15}^{+0.12}(\text{syst.}) \times 10^{20}$	[59,122]
		$0\nu\chi\beta^-\beta^-$ (g.s.)		$>1.6 \times 10^{22}$	[48,122]
		$0\nu\beta^-\beta^-$ (g.s.)	1991.45(1)	$>2.2 \times 10^{25}$	[59,122]
		$0\nu\beta^-\beta^-$ (2_0^+)		$>1.4 \times 10^{23}$	[49,123]
		$2\nu\beta^-\beta^-$ (0_1^+)		$>1.3 \times 10^{24}$	[104,123]
		$0\nu\beta^-\beta^-$ (0_1^+)		$>5.9 \times 10^{24}$	[104,123]
^{128}Te	31.7525(12)	$(0\nu + 2\nu)\beta^-\beta^-$ (all modes)	866.7(7)	$(2.25 \pm 0.09) \times 10^{24}$	[10,108,112]
		$0\nu\beta^-\beta^-$ (g.s.)	$E_{\gamma^*} = 442.9$ keV	$>1.1 \times 10^{23}$	[49,108,112]
		$(0\nu + 2\nu)\beta^-\beta^-$ (2^+)		$>4.7 \times 10^{21}$	[101,112]
^{123}Te	0.8854(6)	EC (g.s.)	51.91(7)	$>9.2 \times 10^{16}$	[108,112,113]
^{120}Te	0.09(1)	$2\nu\beta^+EC$ (g.s.)	1714.81(1.25)	$>7.6 \times 10^{19}$	[121,122,124]
		$0\nu\beta^+EC$ (g.s.)		$>2.7 \times 10^{21}$	[122,124,125]
		$2\nu ECEC$ (g.s.)	$>2.94 \times 10^{15}$	[120,124]	
		$0\nu ECEC$ (g.s.)	$>(1.9-6) \times 10^{18}$	[80,124]	
		$(0\nu + 2\nu)ECEC$ (2^+)	$E_{\gamma^*} = 1171.26$ keV	$>7.5 \times 10^{17}$	[80,124]

Table 2. List of ^{120}Sn β^+EC decay scenarios within Cuoricino detector. For each signature we indicate the particles detected (positron and gammas), the number of bolometers involved and the energy released. If neutrinos are emitted the positron energy is continuous from 0 to $Q_{\beta^+EC} - 2me - E_b$, where $E_b = 30.5$ keV is the K-shell binding energy. Thus, the crystal interested by the decay sees an energy deposition between 30.5 and 692.8 keV. For the 0ν mode in which the e^+ is monochromatic the continuous energy range is replaced by the upper limit, e.g., in scenario (4) the energy released is 1203.8 keV on one crystal, 511 keV on its neighbor.

Signature	Particles Detected	N_{crystals}	Released Energy [keV]
(0)	β^+	1	(30.5, 692.8)
(1)	$\beta^+ + \gamma$	1	(541.5, 1203.8)
(2)	$\beta^+ + \gamma_1 + \gamma_2$	1	(1052.5, 1714.8)
(3)	$\beta^+ + \gamma$	2	(30.5, 692.8), 511
(4)	$\beta^+ + \gamma_1 + \gamma_2$	2	(541.5, 1203.8), 511
(5)	$\beta^+ + \gamma_1 + \gamma_2$	3	(30.5, 692.8), 511, 511

A time window of 100 ms was set for coincidence analysis, and the signatures with the best signal-to-noise ratio were selected. This means scenario (2)–(5) for the 0ν mode and scenario (5) for the 2ν mode.

The most recent result on $0\nu\beta^+EC$ decay of ^{120}Te is the one from the final CUORE-0 data release. In this case, the exposure available was roughly one-half of the Cuoricino one: 35.2 kg·yr of TeO_2 , corresponding to ~ 0.0243 kg·yr of ^{120}Te . However, the combination of an improved background and lower trigger thresholds made it possible to include all the signatures listed in Table 2 in the search thereby increasing the sensitivity. Once no more evidence of a signal was observed and a 90% C.I. limit on the neutrinoless positron emitting electron capture half life of ^{120}Te was set, $T_{1/2}^{0\nu} > 1.6 \times 10^{21}$ yr [125]. The combination of the Cuoricino and CUORE-0 results gives the strongest limit to date on this decay:

$$T_{1/2}^{0\nu\beta^+EC} > 2.7 \times 10^{21} \text{ yr (90\% C.I.)} . \quad (25)$$

A $0\nu\beta^+EC$ decay analysis on CUORE data is currently ongoing. In CUORE, the number of ^{120}Te $\beta\beta$ emitters is $\sim 2.51 \times 10^{21}$ corresponding to a total ^{120}Te mass of ~ 0.5 kg. Given the accumulated exposure of $1 \text{ ton} \cdot \text{yr}$ [70], a factor $\gtrsim 5$ improvement in the sensitivity is foreseen.

^{120}Te has been minimally investigated from the theoretical point of view. At present no calculation of the nuclear matrix elements is available in the literature for the ^{120}Te double beta decay, whereas an improved calculation of the phase space factors for $EC\beta^+$ and $ECEC$ decays for both the 2ν mode and the beyond-SM variant is presented in [25]. Regarding the neutrinoless mode, no theoretical estimates of the half life of $0\nu EC\beta^+$ decay of ^{120}Te are available for comparison with the experimental results. For the 2ν mode only, [126] gives a calculation of the half life. The theoretical value from this reference is 4.4×10^{26} yr.

8. Conclusions

In the framework of the worldwide experimental program to search for neutrinoless double beta decay, the study of tellurium isotopes as potential emitter nuclei has an important role. In this article, we reviewed the past (tracking and geochemical experiments) and current (cryogenic calorimeters, liquid scintillators and semiconductors) experimental techniques employed in the search for $\beta\beta$ decay in Te, pointing out their strengths and limitations in terms of sensitivity, background, energy resolution at the Q-value and sensitivity.

Following an historical approach, we presented the main results obtained for each of the explored isotopes with various experiments. Current (CUORE) and future (SNO+) projects have the study of ^{130}Te decay to the ground state of ^{130}Xe as a primary goal, since it has the highest natural isotopic abundance and its decay mechanism is $\beta^-\beta^-$, which is the least suppressed. However, in recent years a renewed interest towards the alternative $\beta^+\beta^+$, β^+EC and $ECEC$ transitions arose. Double beta decay to the first excited states is also investigated. Moreover, precision measurements of the SM-allowed $2\nu\beta\beta$ decay half life are fundamental as they could help reducing the uncertainty on nuclear matrix elements calculations thereby constraining the effective Majorana mass parameter.

Besides the impressive amount of work done through the past thirty years to extract current measurements and limits on rare tellurium decays, we show that there are still many open questions to be addressed and outdated searches that deserve to be resumed and repeated with large data samples and improved techniques. Among them, we find the analysis of $0\nu\beta\beta$ decay with Majoron emission (Section 4.2), the study of double electron capture decay of ^{120}Te (Section 7) and ^{123}Te (Section 6) single electron capture decay. Regarding the latter, results extracted from past measurements are controversial, and a new measurement could potentially solve this issue. Finally, the search for ^{130}Te decay to the excited states described in Section 4.3 could help fix the large discrepancy between theoretical calculations extracted from different models. ^{128}Te $0\nu\beta\beta$ decay and ^{120}Te $0\nu\beta^+EC$ transition are currently explored with CUORE data, and hopefully improved results will come out. As far as ^{130}Te decay to the ground state is concerned, a comparison with new measurements from the forthcoming SNO+ experiment could validate all the existing results reported here.

Author Contributions: All the authors have actively and equally contributed to the development and writing of this review. All authors have read and agreed to the published version of the manuscript.

Funding: This research received no external funding.

Conflicts of Interest: The authors declare no conflict of interest.

Notes

- 1 Although the half life $T_{1/2}$ is a well defined observable for each emitter nucleus and is related to its full decay rate Γ as $T_{1/2} = \ln 2/\Gamma$, from now on we will refer to the half life of specific processes, replacing the full decay rate in the definition with the one specific to the process of interest.
- 2 Full Width at Half Maximum.
- 3 This result refers to the standard Majoron emission, with spectral index 1.

References

1. Dolinski, M.J.; Poon, A.W.P.; Rodejohann, W. Neutrinoless Double-Beta Decay: Status and Prospects. *Ann. Rev. Nucl. Part. Sci.* **2019**, 219–251. [[CrossRef](#)]
2. Dell’Oro, S.; Marcocci, S.; Viel, M.; Vissani, F. Neutrinoless double beta decay: 2015 review. *Adv. High Energy Phys.* **2016**, 2162659. [[CrossRef](#)]
3. Dell’Oro, S.; Marcocci, S.; Vissani, F. Empirical Inference on the Majorana Mass of the Ordinary Neutrinos. *Phys. Rev. D* **2019**, 073003. [[CrossRef](#)]
4. Menéndez, J. Towards Reliable Nuclear Matrix Elements for Neutrinoless $\beta\beta$ Decay. *JPS Conf. Proc.* **2018**, 012036. [[CrossRef](#)]
5. Engel, J.; Menéndez, J. Status and future of nuclear matrix elements for neutrinoless double-beta decay: A review. *Rep. Prog. Phys.* **2017**, 046301. [[CrossRef](#)] [[PubMed](#)]
6. Suhonen, J.; Civitarese, O. Probing the quenching of g_A by single and double beta decays. *Phys. Lett. B* **2013**, 153–157. [[CrossRef](#)]
7. Brune, T.; Päs, H. Massive Majorons and constraints on the Majoron-neutrino coupling. *Phys. Rev. D* **2019**, 096005. [[CrossRef](#)]
8. Weizsacker, C.F.V. Zur Theorie der Kernmassen. *Z. Phys.* **1935**, 431–458. [[CrossRef](#)]
9. Goeppert-Mayer, M. Double beta-disintegration. *Phys. Rev.* **1935**, 512–516. [[CrossRef](#)]
10. Barabash, A. Precise Half-Life Values for Two-Neutrino Double- β Decay: 2020 Review. *Universe* **2020**, *10*, 159. [[CrossRef](#)]
11. Furry, W.H. On transition probabilities in double beta-disintegration. *Phys. Rev.* **1939**, 1184–1193. [[CrossRef](#)]
12. Buchmüller, W.; Peccei, R.; Yanagida, T. Leptogenesis as the origin of matter. *Annu. Rev. Nucl. Part. Sci.* **2005**, *55*, 311–355. [[CrossRef](#)]
13. Cepedello, R.; Deppisch, F.F.; González, L.; Hati, C.; Hirsch, M. Neutrinoless Double- β Decay with Nonstandard Majoron Emission. *Phys. Rev. Lett.* **2019**, 181801. [[CrossRef](#)] [[PubMed](#)]
14. Ge, S.F.; Lindner, M.; Patra, S. New physics effects on neutrinoless double beta decay from right-handed current. *JHEP* **2015**, 77. [[CrossRef](#)]
15. Deppisch, F.F.; Hirsch, M.; Päs, H. Neutrinoless Double Beta Decay and Physics Beyond the Standard Model. *J. Phys. G* **2012**, 124007. [[CrossRef](#)]
16. Mitra, M.; Senjanovic, G.; Vissani, F. Neutrinoless Double Beta Decay and Heavy Sterile Neutrinos. *Nucl. Phys. B* **2012**, 26–73. [[CrossRef](#)]
17. Tello, V.; Nemevsek, M.; Nesti, F.; Senjanovic, G.; Vissani, F. Left-Right Symmetry: From LHC to Neutrinoless Double Beta Decay. *Phys. Rev. Lett.* **2011**, 151801. [[CrossRef](#)]
18. Mohapatra, R.N.; Pal, P.B. *Massive Neutrinos in Physics and Astrophysics*, 2nd ed.; World Scientific Lecture Notes in Physics; World Scientific: Singapore, 1998; pp. 1–397.
19. Pontecorvo, B. Superweak interactions and double beta decay. *Phys. Lett. B* **1968**, 630–632. [[CrossRef](#)]
20. Feinberg, G.; Goldhaber, M. Microscopic tests of symmetry principles. *Proc. Natl. Acad. Sci. USA* **1959**, *45*, 1301–1312. [[CrossRef](#)] [[PubMed](#)]
21. Particle Data Group. Review of Particle Physics. *Phys. Rev. D* **2018**, 030001. [[CrossRef](#)]
22. Kotila, J.; Iachello, F. Phase space factors for double- β decay. *Phys. Rev. C* **2012**, 034316. [[CrossRef](#)]
23. Barea, J.; Kotila, J.; Iachello, F. Neutrinoless double-positron decay and positron-emitting electron capture in the interacting boson model. *Phys. Rev. C* **2013**, 057301. [[CrossRef](#)]
24. Barea, J.; Kotila, J.; Iachello, F. $0\nu\beta\beta$ and $2\nu\beta\beta$ nuclear matrix elements in the interacting boson model with isospin restoration. *Phys. Rev. C* **2015**, 034304. [[CrossRef](#)]
25. Kotila, J.; Iachello, F. Phase space factors for $\beta^+\beta^+$ decay and competing modes of double- β decay. *Phys. Rev. C* **2013**, 024313. [[CrossRef](#)]
26. Hirsch, M.; Muto, K.; Oda, T.; Klapdor-Kleingrothaus, H.V. Nuclear structure calculation of $\beta^+\beta^+$, β^+/EC and EC/EC decay matrix elements. *Z. Phys. A Hadron. Nucl.* **1994**, *347*, 151–160. [[CrossRef](#)]
27. Meshik, A.P.; Hohenberg, C.M.; Pravdivtseva, O.V.; Kapusta, Y.S. Weak decay of Ba-130 and Ba-132: Geochemical measurements. *Phys. Rev. C* **2001**, 035205. [[CrossRef](#)]
28. Gavriljuk, Y.M.; Gangapshv, A.M.; Kazalov, V.V.; Kuzminov, V.V.; Panasenko, S.I.; Ratkevich, S.S. Indications of $2\nu 2K$ capture in ^{78}Kr . *Phys. Rev. C* **2013**, 035501. [[CrossRef](#)]
29. XENON Collaboration. Observation of two-neutrino double electron capture in ^{124}Xe with XENON1T. *Nature* **2019**, 532–535. [[CrossRef](#)]
30. Blaum, K.; Eliseev, S.; Danevich, F.A.; Tretyak, V.I.; Kovalenko, S.; Krivoruchenko, M.I.; Novikov, Y.N.; Suhonen, J. Neutrinoless Double-Electron Capture. *Rev. Mod. Phys.* **2020**, 045007. [[CrossRef](#)]

31. Sujkowski, Z.; Wycech, S. Neutrinoless double electron capture: A Tool to search for Majorana neutrinos. *Phys. Rev. C* **2004**, 052501. [[CrossRef](#)]
32. Barabash, A.S. Double beta decay experiments. *Phys. Part. Nucl.* **2011**, 613–627. [[CrossRef](#)]
33. Pirinen, P.; Suhonen, J. Systematic approach to β and $2\nu\beta\beta$ decays of mass $A = 100$ –136 nuclei. *Phys. Rev. C* **2015**, 054309. [[CrossRef](#)]
34. Lehnert, B. Excited State Transitions in Double Beta Decay: A brief Review. *EPJ Web Conf.* **2015**, 01025. [[CrossRef](#)]
35. Simkovic, F.; Faessler, A. Distinguishing the $0\nu\beta\beta$ decay mechanisms. *Prog. Part. Nucl. Phys.* **2002**, 201–209. [[CrossRef](#)]
36. Barabash, A.S.; Avignone, F.T., III; Collar, J.I.; Guerard, C.K.; Arthur, R.J.; Brodzinski, R.L.; Miley, H.S.; Reeves, J.H.; Meier, J.R.; Ruddick, K.; et al. Two neutrino double beta decay of Mo-100 to the first excited 0^+ state in Ru-100. *Phys. Lett. B* **1995**, 408–413. [[CrossRef](#)]
37. Barabash, A.S.; Hubert, F.; Hubert, P.; Umatov, V.I. Double beta decay of Nd-150 to the first 0^+ excited state of Sm-150. *JETP Lett.* **2004**, 10–12. [[CrossRef](#)]
38. Belli, P.; Bernabei, R.; Cappella, F.; Caracciolo, V.; Cerulli, R.; Incicchitti, A.; Merlo, V. Double Beta Decay to Excited States of Daughter Nuclei. *Universe* **2020**, 6, 239. [[CrossRef](#)]
39. Chikashige, Y.; Mohapatra, R.N.; Peccei, R.D. Are There Real Goldstone Bosons Associated with Broken Lepton Number? *Phys. Lett. B* **1981**, 265–268. [[CrossRef](#)]
40. Santamaria, A.; Valle, J.W.F. Supersymmetric majoron signatures and solar neutrino oscillations. *Phys. Rev. Lett.* **1988**, 60, 397–400. [[CrossRef](#)]
41. Gelmini, G.; Roncadelli, M. Left-handed neutrino mass scale and spontaneously broken lepton number. *Phys. Lett. B* **1981**, 99, 411–415. [[CrossRef](#)]
42. Cremonesi, O.; Pavan, M. Challenges in Double Beta Decay. *Adv. High Energy Phys.* **2014**, 951432. [[CrossRef](#)]
43. Dassie, D.; Hubert, P.; Isaac, M.C.P.; Izac, C.; Leccia, F.; Mennrath, P.; Longuemare, C.; Blum, D.; Busto, J.; Campagne, J.E.; et al. Double beta decay prototype detector with multiwire drift tubes in the Geiger mode. *Nucl. Instrum. Meth. A* **1991**, 465–475. [[CrossRef](#)]
44. Arnold, R.; Barabash, A.; Blum, D.; Brudanin, V.; Campagne, J.E.; Danevich, F.; Dassié, D.; Egorov, V.; Eschbach, R.; Guyonnet, J.L.; et al. Performance of a prototype tracking detector for double beta decay measurements. *Nucl. Instrum. Meth. A* **1995**, 338–351. [[CrossRef](#)]
45. Arnold, R.; Augier, C.; Bakalyarov, A.M.; Baker, J.; Barabash, A.; Bernaudin, P.; Bouchel, M.; Brudanin, V.; Caffrey, A.J.; Cailleret, J.; et al. Technical design and performance of the NEMO 3 detector. *Nucl. Instrum. Meth. A* **2005**, 79–122. [[CrossRef](#)]
46. Arnold, R.; Augier, C.; Baker, J.; Barabash, A.S.; Basharina-Freshville, A.; Bongrand, M.; Brudanin, V.; Caffrey, A.J.; Cebrián, S.; Chapon, A.; et al. Probing New Physics Models of Neutrinoless Double Beta Decay with SuperNEMO. *Eur. Phys. J. C* **2010**, 927–943. [[CrossRef](#)]
47. Arnold, R.; Augier, C.; Barabash, A.S.; Basharina-Freshville, A.; Birdsall, E.; Blondel, S.; Bongrand, M.; Bourssette, D.; Breier, R.; Brudanin, V.; et al. Measurement of the distribution of ^{207}Bi depositions on calibration sources for SuperNEMO. *arXiv* **2021**, arXiv:2103.14429.
48. Arnold, R.; Augier, C.; Bakalyarov, A.M.; Baker, J.D.; Barabash, A.S.; Basharina-Freshville, A.; Blondel, S.; Blot, S.; Bongrand, M.; Brudanin, V.; et al. Measurement of the Double Beta Decay Half-life of ^{130}Te with the NEMO-3 Detector. *Phys. Rev. Lett.* **2011**, 062504. [[CrossRef](#)] [[PubMed](#)]
49. Arnaboldi, C.; Brofferio, C.; Bucci, C.; Capelli, S.; Cremonesi, O.; Fiorini, E.; Giuliani, A.; Nucciotti, A.; Pavan, M.; Pedretti, M.; et al. A Calorimetric search on double beta decay of Te-130. *Phys. Lett. B* **2003**, 167–175. [[CrossRef](#)]
50. Thomas, H.V.; Patrick, R.A.D.; Crowther, S.A.; Blagburn, D.J.; Gilmour, J.D. Geochemical constraints on the half-life of Te-130. *Phys. Rev. C* **2008**, 054606. [[CrossRef](#)]
51. Inghram, M.G.; Reynolds, J.H. Double beta-decay of Te-130. *Phys. Rev.* **1950**, 822–823. [[CrossRef](#)]
52. Inghram, M.G.; Reynolds, J.H. On the double beta-process. *Phys. Rev.* **1949**, 1265–1266. [[CrossRef](#)]
53. Manuel, O.K. Geochemical Measurements of Double beta Decay. *J. Phys. G* **1991**, S221. [[CrossRef](#)]
54. Takaoka, N.; Ogata, K. The Half-life of ^{130}Te Double β -decay. *Z. Nat. A* **1966**, 84–90. [[CrossRef](#)]
55. Takaoka, N.; Motomura, Y.; Nagao, K. Half-life of Te-130 double-beta decay measured with geologically qualified samples. *Phys. Rev. C* **1996**, 1557–1561. [[CrossRef](#)]
56. Kirsten, T.; Heusser, E.; Kaether, D.; Oehm, J.; Pernicka, E.; Richter, H. New geochemical double beta decay measurements on various selenium ores and remarks concerning tellurium isotopes. In Proceedings of the International Symposium on Nuclear Beta Decays and Neutrino: Neutrino Mass and $V+A$ Interaction in Particle and Nuclear Physics, Osaka, Japan, 11–13 June 1986; pp. 81–92.
57. Bernatowicz, T.; Brannon, J.; Brazzle, R.; Cowsik, R.; Hohenberg, C.; Podosek, F. Precise determination of relative and absolute beta beta decay rates of Te-128 and Te-130. *Phys. Rev. C* **1993**, 806–825. [[CrossRef](#)] [[PubMed](#)]
58. Meshik, A.P.; Hohenberg, C.M.; Pravdivtseva, O.V.; Bernatowicz, T.J.; Kapusta, Y.S. Te-130 and Te-128 double beta decay half-lives. *Nucl. Phys. A* **2008**, 275–289. [[CrossRef](#)]
59. Adams, D.Q.; Alduino, C.; Alfonso, K.; Avignone, F.T.; Azzolini, O.; Bari, G.; Bellini, F.; Benato, G.; Biassoni, M.; Branca, A.; et al. Measurement of the $2\nu\beta\beta$ Decay Half-Life of ^{130}Te with CUORE. *Phys. Rev. Lett.* **2021**, 171801. [[CrossRef](#)] [[PubMed](#)]
60. Enss, C. (Ed.) *Cryogenic Particle Detection*; Springer: Berlin/Heidelberg, Germany, 2005. [[CrossRef](#)]

61. CUORE Collaboration. Improved Limit on Neutrinoless Double-Beta Decay in ^{130}Te with CUORE. *Phys. Rev. Lett.* **2020**, 122501. [[CrossRef](#)]
62. CUPID-Mo Collaboration. New Limit for Neutrinoless Double-Beta Decay of ^{100}Mo from the CUPID-Mo Experiment. *Phys. Rev. Lett.* **2021**, 181802. [[CrossRef](#)]
63. Armatol, A.; Armengaud, E.; Armstrong, W.; Augier, C.; Avignone, F.T., III; Azzolini, O.; Bandac, I.C.; Barabash, A.S.; Bari, G.; Barresi, A.; et al. A CUPID Li_2 $^{100}\text{MoO}_4$ scintillating bolometer tested in the CROSS underground facility. *Jinst* **2021**, P02037. [[CrossRef](#)]
64. Azzolini, O.; Beeman, J.W.; Bellini, F.; Beretta, M.; Biassoni, M.; Brofferio, C.; Bucci, C.; Capelli, S.; Cardani, L.; Carniti, P.; et al. Final result of CUPID-0 phase-I in the search for the ^{82}Se Neutrinoless Double- β Decay. *Phys. Rev. Lett.* **2019**, 032501. [[CrossRef](#)] [[PubMed](#)]
65. Brofferio, C.; Dell’Oro, S. Contributed Review: The saga of neutrinoless double beta decay search with TeO_2 thermal detectors. *Rev. Sci. Instrum.* **2018**, 121502. [[CrossRef](#)]
66. Arnaboldi, C.; Avignone, F.T., III; Beeman, J.; Barucci, M.; Balata, M.; Brofferio, C.; Bucci, C.; Cebrian, S.; Creswick, R.J.; Capelli, S.; et al. CUORE: A Cryogenic underground observatory for rare events. *Nucl. Instrum. Meth. A* **2004**, 775–798. [[CrossRef](#)]
67. Artusa, D.R.; Avignone, F.T.; Azzolini, O.; Balata, M.; Banks, T.I.; Bari, G.; Beeman, J.; Bellini, F.; Bersani, A.; Biassoni, M.; et al. Searching for neutrinoless double-beta decay of ^{130}Te with CUORE. *Adv. High Energy Phys.* **2015**, 879871. [[CrossRef](#)]
68. CUORE Collaboration. Search for Neutrinoless Double-Beta Decay of ^{130}Te with CUORE-0. *Phys. Rev. Lett.* **2015**, 102502. [[CrossRef](#)]
69. Andreotti, E.; Arnaboldi, C.; Avignone, F.T., III; Balata, M.; Bandac, I.; Barucci, M.; Beeman, J.W.; Bellini, F.; Brofferio, C.; Bryant, A.; et al. ^{130}Te Neutrinoless Double-Beta Decay with CUORICINO. *Astropart. Phys.* **2011**, 822–831. [[CrossRef](#)]
70. Adams, D.Q.; Alduino, C.; Alfonso, K.; Avignone, F.T., III; Azzolini, O.; Bari, G.; Bellini, F.; Benato, G.; Beretta, M.; Biassoni, M.; et al. High sensitivity neutrinoless double-beta decay search with one tonne-year of CUORE data. *arXiv* **2021**, arXiv:2104.06906.
71. Armstrong, W.R.; Chang, C.; Hafidi, K.; Lisovenko, M.; Novosad, V.; Pearson, J.; Polakovic, T.; Wang, G.; Yefremenko, V.; Zhang, J.; et al. CUPID pre-CDR. *arXiv* **2019**, arXiv:1907.09376.
72. Alduino, C.; Alfonso, K.; Artusa, D.R.; Avignone, F.T., III; Azzolini, O.; Banks, T.I.; Bari, G.; Beeman, J.W.; Bellini, F.; Benato, G.; et al. CUORE sensitivity to $0\nu\beta\beta$ decay. *Eur. Phys. J. C* **2017**, 532. [[CrossRef](#)]
73. KamLAND-Zen Collaboration. Search for Majorana Neutrinos near the Inverted Mass Hierarchy Region with KamLAND-Zen. *Phys. Rev. Lett.* **2016**, 082503. [[CrossRef](#)]
74. Andringa, S.; Arushanova, E.; Asahi, S.; Askins, M.; Auty, D.J.; Back, A.R.; Barnard, Z.; Barros, N.; Beier, E.W.; Bialek, A.; et al. Current Status and Future Prospects of the SNO+ Experiment. *Adv. High Energy Phys.* **2016**, 6194250. [[CrossRef](#)]
75. SNO Collaboration. Direct evidence for neutrino flavor transformation from neutral current interactions in the Sudbury Neutrino Observatory. *Phys. Rev. Lett.* **2002**, 011301. [[CrossRef](#)]
76. SNO Collaboration. Measurement of the Cosmic Ray and Neutrino-Induced Muon Flux at the Sudbury Neutrino Observatory. *Phys. Rev. D* **2009**, 012001. [[CrossRef](#)]
77. O’Keefe, H.M.; O’Sullivan, E.; Chen, M.C. Scintillation decay time and pulse shape discrimination in oxygenated and deoxygenated solutions of linear alkylbenzene for the SNO+ experiment. *Nucl. Instrum. Meth. A* **2011**, 119–122. [[CrossRef](#)]
78. Caravaca, J. SNO+ status and prospects. *Int. J. Mod. Phys. A* **2020**, 2044013. [[CrossRef](#)]
79. Paton, J. Neutrinoless Double Beta Decay in the SNO+ Experiment. Prospects in Neutrino Physics. *arXiv* **2019**, arXiv:1904.01418.
80. Barabash, A.; Hubert, F.; Hubert, P.; Umatov, V. New limits on the beta+ EC and ECEC processes in Te-120. *J. Phys. G* **2007**, 1721–1728. [[CrossRef](#)]
81. GERDA Collaboration. Final Results of GERDA on the Search for Neutrinoless Double- β Decay. *Phys. Rev. Lett.* **2020**, 252502. [[CrossRef](#)]
82. Ebert, J.; Fritts, M.; Gehre, D.; Gößling, C.; Göpfert, T.; Hagner, C.; Heidrich, N.; Klingenberg, R.; Köttig, T.; Kröninger, K.; et al. The COBRA demonstrator at the LNGS underground laboratory. *Nucl. Instrum. Meth. A* **2016**, 114–120. [[CrossRef](#)]
83. Ebert, J.; Fritts, M.; Gehre, D.; Gößling, C.; Hagner, C.; Heidrich, N.; Klingenberg, R.; Kröninger, K.; Nitsch, C.; Oldorf, C.; et al. Results of a search for neutrinoless double- β decay using the COBRA demonstrator. *Phys. Rev. C* **2016**, 024603. [[CrossRef](#)]
84. Suhonen, J.; Civitarese, O. Weak-interaction and nuclear-structure aspects of nuclear double beta decay. *Phys. Rep.* **1998**, 123–214. [[CrossRef](#)]
85. Faessler, A.; Simkovic, F. Double beta decay. *J. Phys. G Nucl. Part. Phys.* **1998**, 24, 2139. [[CrossRef](#)]
86. Simkovic, F.; Domin, P.; Semenov, S.V. The Single state dominance hypothesis and the two neutrino double beta decay of Mo-100. *J. Phys. G* **2001**, 2233–2240. [[CrossRef](#)]
87. Zdesenko, Y.G. On lepton charge conservation in the double β decay of ^{130}Te . *JETP Lett.* **1980**, 32, 58.
88. Alessandrello, A.; Brofferio, C.; Camin, D.V.; Cremonesi, O.; Fiorini, E.; Gervasio, G.; Giuliani, A.; Nucciotti, A.; Pavan, M.; Pessina, G.; et al. Milano experiment on $0\nu\beta\beta$ decay of Te-130 with a thermal detector. *Nucl. Phys. B Proc. Suppl.* **1993**, 83–87. [[CrossRef](#)]
89. Kirsten, T.; Richter, H.; Jessberger, E. Rejection of evidence for nonzero neutrino rest mass from double beta decay. *Phys. Rev. Lett.* **1983**, 474–477. [[CrossRef](#)]
90. Alessandrello, A.; Brofferio, C.; Camin, D.; Cremonesi, O.; Fiorini, E.; Garcia, E.; Giuliani, A.; de Marcillac, P.; Nucciotti, A.; Pavan, M.; et al. A new search for neutrinoless $\beta\beta$ decay with a thermal detector. *Phys. Lett. B* **1994**, 335, 519–525. [[CrossRef](#)]

91. Alessandrello, A.; Brofferio, C.; Cremonesi, O.; Fiorini, E.; Giuliani, A.; Nucciotti, A.; Pavan, M.; Pirro, S.; Pessina, G.; Parmeggiano, S.; et al. A massive thermal detector for alpha and gamma spectroscopy. *Nucl. Instrum. Meth. A* **2000**, 397–402. [[CrossRef](#)]
92. Alduino, C.; Alfonso, K.; Artusa, D.R.; Avignone, F.T., III; Azzolini, O.; Balata, M.; Banks, T.I.; Bari, G.; Beeman, J.W.; Bellini, F.; et al. CUORE-0 detector: Design, construction and operation. *J. Instrum.* **2016**, P07009. [[CrossRef](#)]
93. Arnaboldi, C.; Brofferio, C.; Bryant, A.; Bucci, C.; Canonica, L.; Capelli, S.; Carrettoni, M.; Clemenza, M.; Dafinei, I.; Di Domizio, S.; et al. Production of high purity TeO₂ single crystals for the study of neutrinoless double beta decay. *J. Cryst. Growth* **2010**, 2999–3008. [[CrossRef](#)]
94. Alessandria, F.; Ardito, R.; Artusa, D.R.; Avignone, F.T., III; Azzolini, O.; Balata, M.; Banks, T.I.; Bari, G.; Beeman, J.; Bellini, F.; et al. Validation of techniques to mitigate copper surface contamination in CUORE. *Astropart. Phys.* **2013**, 13–22. [[CrossRef](#)]
95. Buccheri, E.; Capodiferro, M.; Morganti, S.; Orio, F.; Pelosi, A.; Pettinacci, V. An assembly line for the construction of ultra-radio-pure detectors. *Nucl. Instrum. Meth. A* **2014**, 130–140. [[CrossRef](#)]
96. CUORE Collaboration. Analysis techniques for the evaluation of the neutrinoless double- β decay lifetime in ¹³⁰Te with the CUORE-0 detector. *Phys. Rev. C* **2016**, 045503. [[CrossRef](#)]
97. CUORE Collaboration. First Results from CUORE: A Search for Lepton Number Violation via $0\nu\beta\beta$ Decay of ¹³⁰Te. *Phys. Rev. Lett.* **2018**, 132501. [[CrossRef](#)]
98. Campani, A.; Adams, D.Q.; Alduino, C.; Alfonso, K.; Avignone, F.T., III; Azzolini, O.; Bari, G.; Bellini, F.; Benato, G.; Biassoni, M.; et al. Lowering the Energy Threshold of the CUORE Experiment: Benefits in the Surface Alpha Events Reconstruction. *J. Low Temp. Phys.* **2020**, 321–330. [[CrossRef](#)]
99. Alduino, C.; Alfonso, K.; Artusa, D.R.; Avignone, F.T., III; Azzolini, O.; Bari, G.; Beeman, J.W.; Bellini, F.; Benato, G.; Bersani, A.; et al. Low Energy Analysis Techniques for CUORE. *Eur. Phys. J. C* **2017**, 857. [[CrossRef](#)]
100. Huang, R.; Armengaud, E.; Augier, C.; Barabash, A.S.; Bellini, F.; Benato, G.; Benoît, A.; Beretta, M.; Bergé, L.; Billard, J.; et al. Pulse shape discrimination in CUPID-Mo using principal component analysis. *J. Instrum.* **2021**, 16, P03032. [[CrossRef](#)]
101. Bellotti, E.; Cattadori, C.; Cremonesi, O.; Fiorini, E.; Liguori, C.; Pullia, A.; Sverzellati, P.P.; Zanotti, L. A Search for Double Beta Decay of ¹²⁸Te and ¹³⁰Te Leading to the First Excited State of Daughter Nuclei. *Europhys. Lett.* **1987**, 889–893. [[CrossRef](#)]
102. Andreotti, E.; Arnaboldi, C.; Avignone, F.T.; Balata, M.; Bandac, I.; Barucci, M.; Beeman, J.W.; Bellini, F.; Brofferio, C.; Bryant, A.; et al. Double-beta decay of ¹³⁰Te to the first 0⁺ excited state of ¹³⁰Xe with CUORICINO. *Phys. Rev. C* **2012**, 045503. [[CrossRef](#)]
103. Alduino, C.; Alfonso, K.; Artusa, D.R.; Avignone, F.T., III; Azzolini, O.; Banks, T.I.; Bari, G.; Beeman, J.W.; Bellini, F.; Bersani, A.; et al. Double-beta decay of ¹³⁰Te to the first 0⁺ excited state of ¹³⁰Xe with CUORE-0. *Eur. Phys. J. C* **2019**, 795. [[CrossRef](#)]
104. CUORE Collaboration. Search for Double-Beta Decay of ¹³⁰Te to the 0⁺ States of ¹³⁰Xe with CUORE. *Eur. Phys. J. C* **2021**. [[CrossRef](#)]
105. Suhonen, J.; Civitarese, O. Single and double beta decays in the A = 100, A = 116 and A = 128 triplets of isobars. *Nucl. Phys. A* **2014**, 1–23. [[CrossRef](#)]
106. Barea, J.; Kotila, J.; Iachello, F. Nuclear matrix elements for double- β decay. *Phys. Rev. C* **2013**, 014315. [[CrossRef](#)]
107. Barabash, A.S. Precise half-life values for two neutrino double beta decay. *Phys. Rev. C* **2010**, 035501. [[CrossRef](#)]
108. Wang, M.; Huang, W.J.; Kondev, F.G.; Audi, G.; Naimi, S. The AME 2020 atomic mass evaluation (II). Tables, graphs and references. *Chin. Phys. C* **2021**, 030003. [[CrossRef](#)]
109. Alduino, C.; Alfonso, K.; Artusa, D.R.; Avignone, F.T., III; Azzolini, O.; Banks, T.I.; Bari, G.; Beeman, J.W.; Bellini, F.; Bersani, A.; et al. Measurement of the two-neutrino double-beta decay half-life of ¹³⁰Te with the CUORE-0 experiment. *Eur. Phys. J. C* **2017**, 13. [[CrossRef](#)]
110. Nutini, I.; Adams, D.Q.; Alduino, C.; Alfonso, K.; Avignone, F.T., III; Azzolini, O.; Bari, G.; Bellini, F.; Benato, G.; Biassoni, M.; et al. The CUORE Detector and Results. *J. Low Temp. Phys.* **2020**, 519–528. [[CrossRef](#)]
111. Deppisch, F.; Pas, H. Pinning down the mechanism of neutrinoless double beta decay with measurements in different nuclei. *Phys. Rev. Lett.* **2007**, 232501. [[CrossRef](#)] [[PubMed](#)]
112. Fehr, M.A.; Rehkamper, M.; Halliday, A.N. Application of MC-ICPMS to the precise determination of tellurium isotope compositions in chondrites, iron meteorites and sulfides. *Int. J. Mass Spectrom.* **2004**, 232, 83–94. [[CrossRef](#)]
113. Alessandrello, A.; Arnaboldi, C.; Brofferio, C.; Capelli, S.; Cremonesi, O.; Fiorini, E.; Nucciotti, A.; Pavan, M.; Pessina, G.; Pirro, S.; et al. New limits on naturally occurring electron capture of Te-123. *Phys. Rev. C* **2003**, 014323. [[CrossRef](#)]
114. Alessandria, F.; Ardito, R.; Artusa, D.R.; Avignone, F.T., III; Azzolini, O.; Balata, M.; Banks, T.I.; Bari, G.; Beeman, J.; Bellini, F.; et al. The low energy spectrum of TeO₂ bolometers: Results and dark matter perspectives for the CUORE-0 and CUORE experiments. *Jcap* **2013**, 38. [[CrossRef](#)]
115. Bianchetti, M.; Quaglia, M.R.; Colò, G.; Pizzochero, P.M.; Broglia, R.A.; Bortignon, P.F. Competition between Particle Hole and Particle-Particle Correlations in Forbidden Electron Capture: The Case of Te-123. *Phys. Rev. C* **1997**, 56, R1675(R). [[CrossRef](#)]
116. Watt, D.E.; Glover, R.N. A search for radioactivity among the naturally occurring isobaric pairs. *Philos. Mag.* **1962**, 7, 105–114. [[CrossRef](#)]
117. Alessandrello, A.; Brofferio, C.; Camin, D.V.; Caspani, P.; Colling, P.; Cremonesi, O.; Fiorini, E.; Giuliani, A.; Nucciotti, A.; Pavan, M.; et al. Evidence for Naturally Occurring Electron Capture of Te-123. *Phys. Rev. Lett.* **1996**, 3319–3322. [[CrossRef](#)]
118. Dawson, J.; Goessling, C.; Janutta, B.; Junker, M.; Koettig, T.; Muenstermann, D.; Rajek, S.; Reeve, C.; Schulz, O.; Wilson, J.R.; et al. Experimental study of double beta decay modes using a CdZnTe detector array. *Phys. Rev. C* **2009**, 025502. [[CrossRef](#)]

119. Bloxham, T.; Boston, A.; Dawson, J.; Dobos, D.; Fox, S.P.; Freer, M.; Fulton, B.R.; Gößling, C.; Harrison, P.F.; Junker, M.; et al. First results on double beta decay modes of Cd, Te and Zn isotopes with the COBRA experiment. *Phys. Rev. C* **2007**, 025501. [[CrossRef](#)]
120. Kiel, H.; Munstermann, D.; Zuber, K. A Search for various double beta decay modes of Cd, Te and Zn isotopes. *Nucl. Phys. A* **2003**, 499–514. [[CrossRef](#)]
121. Andreotti, E.; Arnaboldi, C.; Avignone, F.T., III; Balata, M.; Bandac, I.; Barucci, M.; Beeman, J.W.; Bellini, F.; Brofferio, C.; Bryant, A.; et al. Search for beta plus/EC double beta decay of ^{120}Te . *Astropart. Phys.* **2011**, 643–648. [[CrossRef](#)]
122. Scielzo, N.D.; Caldwell, S.; Savard, G.; Clark, J.A.; Deibel, C.M.; Fallis, J.; Gulick, S.; Lascar, D.; Levand, A.F.; Li, G.; et al. Double- β decay Q values of ^{130}Te , ^{128}Te , and ^{120}Te . *Phys. Rev. C* **2009**, 025501. [[CrossRef](#)]
123. Singh, B. Nuclear Data Sheets for $A = 130$. *Nucl. Data Sheets* **2001**, 33–242. [[CrossRef](#)]
124. Meija, J.; Coplen, T.B.; Berglund, M.; Brand, W.A.; De Bièvre, P.; Gröning, M.; Holden, N.E.; Irrgeher, J.; Loss, R.D.; Walczyk, T.; et al. Isotopic compositions of the elements 2013 (IUPAC Technical Report). *Pure Appl. Chem.* **2016**, 293–306. [[CrossRef](#)]
125. CUORE Collaboration. Search for Neutrinoless $\beta^+\text{EC}$ Decay of ^{120}Te with CUORE-0. *Phys. Rev. C* **2018**, 055502. [[CrossRef](#)]
126. Abad, J.; Morales, A.; Núñez-Lagos, R.; Pacheco, A. An estimation of the rates of (two-neutrino) double beta decay and related processes. *J. Phys. Colloq.* **1984**, 45. [[CrossRef](#)]